THE ASTROPHYSICAL JOURNAL, 161:587–617, August 1970

METAL-POOR STARS. III. ON THE EVOLUTION OF HORIZONTAL-BRANCH STARS*

ICKO IBEN, JR., AND ROBERT T. ROOD†
Massachusetts Institute of Technology
Received 1969 November 17; revised 1970 March 16

ABSTRACT

We describe the evolution of low-mass stars of composition $Y = 0.1, 0.2, 0.3$ and $\log Z = -3, -4$ during the phase of core helium burning. Several models for $Y = 0.3$ are evolved until a large carbon-oxygen core develops. By comparing properties of giant-branch and horizontal-branch models with the observations, we find that $Y \sim 0.29 \pm 0.05$ best describes cluster stars if $Z = 10^{-3}$–10^{-4}. For such compositions, model tracks during core helium burning are all quite short compared with the color width of horizontal branches appearing in nature. We conclude that there may be a spread in stellar mass along the horizontal branch that is of the order of 0.1–0.2 $M_{\odot}$. We show that if the mass distribution is continuous, the horizontal branch will define a solid wedge in the color-magnitude diagram, regardless of whether or not an individual track exhibits a blueward hook. Using current estimates of the initial mass of the helium core when losses due to plasma neutrinos are included, we estimate ages for M3, M92, and M15 to be on the order of 11–13 billion years. RR Lyrae luminosities are consistent with those given by the method of statistical parallax and are only slightly larger than those currently suggested by pulsation theory when fitted to the observations. We infer that most of an observed rate of period change dP/dt for RR Lyrae stars is "noise." The distinct bias toward positive values of dP/dt in ω Cen and the small value of $\langle dP/dt \rangle$ in M3 can be interpreted as evidence that stars in M3 pass through the instability strip during the major phase of core helium burning and hence have high Z, whereas stars in ω Cen pass through the strip rapidly from blue to red toward the end of core helium burning and hence have low Z. Finally, we identify the secondary or asymptotic giant branch in globular clusters as the residence of stars that are burning helium in a shell outside a carbon-oxygen core. These stars evolve upward and to the red in the H-R diagram.

I. INTRODUCTION AND SUMMARY OF RESULTS

The general features of evolution through the horizontal-branch phase have been outlined in previous papers (Faulkner and Iben 1966; Iben and Faulkner 1968; Rood and Iben 1968) which describe the dependence of evolutionary-track topology on (1) initial mass of the helium core, (2) total stellar mass, and (3) helium abundance Y in the envelope.

In this paper, we examine the dependence of evolutionary-track characteristics during core helium burning on the heavy-element abundance parameter Z. We also describe the behavior of evolutionary tracks for more complete ranges in stellar mass and in the Y-coordinate than heretofore and devote attention to the time dependence of several interior-structure variables. Finally, we describe the evolution of several models after helium has been exhausted at their centers and show that the tracks of models with two shell sources define an "asymptotic" branch that has an analogue in real clusters.

Input physics has been described in Paper I (Iben and Rood 1970), and initial horizontal-branch models have been described in Paper II (Rood 1970). The major improvement over earlier work is the incorporation of Cox-Stewart (1970) opacities. These opacities do not include the improvements discussed by Watson (1969*a*, *b*). The correction to the electron-scattering contribution discussed by Watson is negligible over most of the models considered, becoming on the order of 10 percent only near the hydrogen-burning shell.

* Supported in part by the National Science Foundation (GP-8060, GP-11277) and in part by the National Aeronautics and Space Administration (NGL 22-009-019).

† Supported in part by the Alfred P. Sloan Foundation Basic Research Fund at M.I.T.

As was shown in Paper II, the new opacities lead to a substantial reduction in the luminosity level of the zero-age horizontal branch (ZAHB) defined by models of different total mass but of the same initial helium-core mass and of the same envelope composition. We find that this reduction in luminosity persists during the entire phase of core helium burning with the consequence that our present estimates are in accord with estimates of the absolute luminosity of RR Lyrae stars as given by the method of statistical parallax. They are still somewhat higher than those given by pulsation theory in conjunction with statistical properties of RR Lyrae stars in globular clusters. A major consequence of the reduced luminosity is an increase by approximately 3 billion years in all derived cluster ages.

The correlation between track topology and the envelope-helium abundance parameter Y does not change from that established earlier. For each choice of Z there exists a critical $Y = Y_I(Z)$ such that, when $Y < Y_I$, models all evolve to the red. When $Y > Y_I$, models can evolve to the blue for a portion of their core-helium-burning lives. The larger Y is relative to Y_I, the longer relative time does a model spend evolving to the blue. We can estimate that $Y_I \sim 0.28$ when $Z = 10^{-4}$ and $Y_I \sim 0.25$ when $Z = 10^{-3}$.

We find that for no presently allowable choices of Y, Z, and initial helium-core mass does the evolutionary track during core helium burning for an individual model cover a range in the color coordinate that is comparable with the observed spread in color along the horizontal branch in many clusters. In fact, for the values of Y and Z most favored ($Y \gtrsim Y_I$, $Z = 10^{-3} \rightarrow 10^{-4}$), individual tracks are the stubbiest. We can account for the observed spread in color along the horizontal branch by accepting that there is also a spread in stellar mass along this branch, bluer stars being less massive (on the average) and less luminous than redder stars. It is somewhat sobering to realize that this conclusion comes near the end of an investigation that has for several years relied heavily on aesthetic arguments against mass loss and has been guided by the expectation of obtaining, as a final result, individual tracks whose color amplitudes equal the entire spread in color along observed horizontal branches.

The masses and luminosities we assign to RR Lyrae stars are still somewhat larger than those estimated on the basis of a comparison between pulsation theory and the observations. We remark that (1) the uncertainties involved in the opacities most pertinent to envelope pulsation are quite different from those involved in the opacities most pertinent to interior structure and (2) the comparison between the results of pulsation theory and the observations requires knowledge of an uncertain transformation between observed color and theoretical surface temperature.

We have carried several models beyond the phase of core helium burning well into the phase when both hydrogen and helium burn in shells. In the H-R diagram, the evolutionary tracks of models with two shell sources begin at a luminosity that is roughly 0.5 mag brighter than that of the average model of the same color that is burning helium in the core. The tracks of those models that are sufficiently massive then approach the red-giant branch asymptotically. The helium-burning shell almost reaches the hydrogen shell in a time that is roughly from two-thirds to four-fifths of the time spent by a model in the phase of core helium burning. Just as one can construct a theoretical horizontal branch from core-helium-burning models, so one can construct an "asymptotic" branch from those models with a double shell source that approach the giant branch. This asymptotic branch has a direct counterpart in real clusters.

In our concluding section, we investigate the possibility that an additional constraint on theoretical models is imposed by the apparently secular changes in period that have been derived for RR Lyrae stars in several clusters. We find that the rate at which a model of any composition passes from red to blue through the RR Lyrae strip during core helium burning is an order of magnitude slower than that inferred from a typical estimated negative rate of period change when it is assumed that the observed rate is a direct measure of the speed of structural changes caused by nuclear burning in the deep interior. The slow change in envelope structure occasioned by nuclear burning in the interior is therefore not responsible for the bulk of a derived change in period. Tentatively considering the major component of an average rate of change in period to be random "noise," we suggest that it is marginally possible that information about evolutionary changes can be obtained after subtraction of the noise. As an example, we show that the difference between M3 and ω Cen in the distribution of number versus rate of change in period can be understood in terms of differences in the evolutionary behavior of stars in the two clusters brought about by differences in metal abundance.

II. PRELIMINARY COMMENTS ON THE INITIAL DISTRIBUTION OF ELEMENTS

Our assumption that the total number of heavy elements per gram is the same throughout the star deserves comment. Prior to the helium flash, matter in the helium core is compacted within a sphere of radius roughly 0.03 $R_\odot$, a size that is nearly independent of envelope composition and core mass (Iben 1968). Core mass reaches roughly 0.5 $M_\odot$ just before the flash, so the self-gravitational binding energy of the core is then approximately $G(M_\odot/2)^2/(0.03\ R_\odot) \sim 3 \times 10^{49}$ ergs. The total kinetic energy of the degenerate electrons in the core is approximately one-half of the gravitational binding energy or $\sim\frac{3}{2} \times 10^{49}$ ergs. Since the core can expand appreciably only when kT per electron becomes of the order of the average energy of an electron prior to the flash, on the order of $\frac{3}{2} \times 10^{49}$ ergs in the form of thermal energy must be supplied by nuclear reactions during the flash. Since there are about $\frac{3}{2} \times 10^{56}$ α-particles in a 0.5 $M_\odot$ core and since 3.89×10^{-6} ergs are released per α-particle in the formation of a ^{12}C nucleus, a reservoir of about 6×10^{50} ergs is available for lifting core degeneracy. Since this is about 40 times what is necessary, we conclude that, in order of magnitude, only 2 or 3 percent of the core mass will be converted into ^{12}C during the flash.

How this ^{12}C is distributed within the star after the flash is not as easily answered. Quasi-static calculations that neglect neutrino losses via the plasma process (Schwarzschild and Härm 1962, 1964, 1966) suggest that, after the peak of the flash, convection mixes matter over most of the region between the center and the hydrogen-burning shell, but does not extend to the hydrogen shell.

One quasi-static calculation which includes neutrino losses (Thomas 1967) suggests that the flash consists of a sequence of bursts in a shell that gradually eats its way toward the center, leaving behind a fairly uniform distribution of ^{12}C at an abundance of a few percent by mass. Thomas also finds that some ^{12}C is carried into the envelope following the first shell flash. If subsequent investigation bears out this result, then many of the conclusions in this paper may require modification.

As Sugimoto (1964) has shown, if convective transport in the core is sufficiently inefficient, the flash could be dynamically explosive. A detailed dynamic calculation by Edwards (1970) verifies that, with an appropriate treatment of time-dependent convection, the flash can be dynamic and, in addition, shows that extensive mixing between flash products and hydrogen-rich matter beyond the shell can occur. If the flash is explosive, one might also expect a variation in final helium-core mass from star to star, even if initial composition and mass do not vary. Significant mass loss due to shocks generated in the exploding core could also occur (Ono and Sakashita 1961; Sakashita and Tanaka 1962; Ohyama 1963).

For lack of conclusive evidence to the contrary, we adopted the simplest course in assuming that the flash is not dynamically explosive and that the end results of the Schwarzschild and Härm quasi-static calculations are correct whether or not neutrino losses occur. With this assumption it remains, then, only to ask whether some ^{12}C evenly distributed (at an abundance of 2 or 3 percent by mass) between the center of the convective core and the hydrogen shell of an initial horizontal-branch model will affect the position of the model in the H-R diagram and its subsequent evolution. Part of the answer is that, since electron scattering is the dominant source of opacity over much of the core, the opacity is essentially unaffected by increasing the ^{12}C abundance to a few percent. Further, such an increase in the ^{12}C abundance does not alter the molecular weight by an appreciable amount. The tentative conclusion that an admixture of a few percent of ^{12}C to an otherwise pure ^4He core does not alter model behavior in any essential respect has been checked by direct calculations (Paper II).

III. EVOLUTIONARY TRACKS AND LIFETIMES

a) *Track Topology during Core Helium Burning*

Figure 1, *a–d*, shows evolutionary paths of the core-helium-burning models studied. All combinations of envelope-composition variables formed from $Z_e = 10^{-4}$, 10^{-3} and $Y_e = 0.1$, 0.2, 0.3 are represented. The range Y has been terminated at 0.3 on the strength of limits estimated in earlier work. Hopefully the range in Z is representative of stars in many globular clusters. For each choice of composition, core masses have been chosen to approximately span the sets suggested by recent investigations of model stars at the red-giant tip (Thomas 1967; Eggleton 1968; Iben 1968).

In the figures, each dashed line labeled ZAHB defines the locus of initial horizontal-branch models that have the same helium-core mass M_C. Solid curves punctuated by tick marks are evolutionary tracks. Two adjacent tick marks are separated by a time interval of 5×10^6 yr. Total model mass M (in units of $M_\odot$) is indicated beside each initial model that has been evolved, and the initial ratio of helium core luminosity to total luminosity is indicated in parentheses.

All models for $Y < 0.2$ evolve to the red, regardless of what value of Z is chosen and regardless of model core mass and total mass (in the ranges thought appropriate for understanding the horizontal branches in globular clusters).

When $Y = 0.30$, the fractional time spent by a model evolving to the blue and the total color range of the blueward path depend on Z and upon core mass and total mass as well. For models that do not develop a large convective envelope during core helium burning, the relative duration and/or the color range of blueward and redward motion can be discussed in terms of a single parameter, either the ratio of the luminosity L_{He} of the helium-burning core to the luminosity L_H of the hydrogen-burning shell or the ratio $L_{He}/(L_H + L_{He}) = L_{He}/L$. The larger the relative contribution of the shell to escaping energy, the greater the tendency for evolution toward the blue. If the parameter L_{He}/L is less than about 0.425 in the initial model, then the model is sure to evolve to the blue during some portion of its core-helium-burning lifetime. If $L_{He}/L > 0.55$ in the initial model, then no evolution to the blue will occur, except for a brief phase following the exhaustion of helium at the center. It is an easy matter to understand how this one parameter depends on M_C and M.

The other parameter of interest is M_e, the mass in the convective envelope. All other things being equal, the larger M_e, the more abbreviated is the color range traversed during blueward evolution. Envelope mass becomes appreciable in initial models lying along the upward-curving portion of the ZAHB. The redder the model star along this curved portion, the larger is M_e and the more foreshortened is the evolutionary track.

For a given initial core mass, the *path length* of the blueward motion is much more sensitive to the ratio L_{He}/L than is the *duration* t_B of the blueward motion. This is illustrated by the tracks for $M_C = 0.475\ M_\odot$ in Figure 1, both *a* and *b*. As stellar mass increases, track length first increases and then, beyond some critical mass, decreases as envelope convection becomes progressively more important. And yet t_B remains fairly constant. Thus, although the correlation between the blueward track length and the value of L_{He}/L_H is replaced by an inverse correlation between blueward track length and M_e, the correlation between t_B and L_{He}/L is nearly unaffected.

b) *Lifetimes during Core Helium Burning*

A recently devised procedure for estimating the initial helium abundance of stars in globular clusters (Iben 1968; Iben and Rood 1969) requires a knowledge of "horizontal-

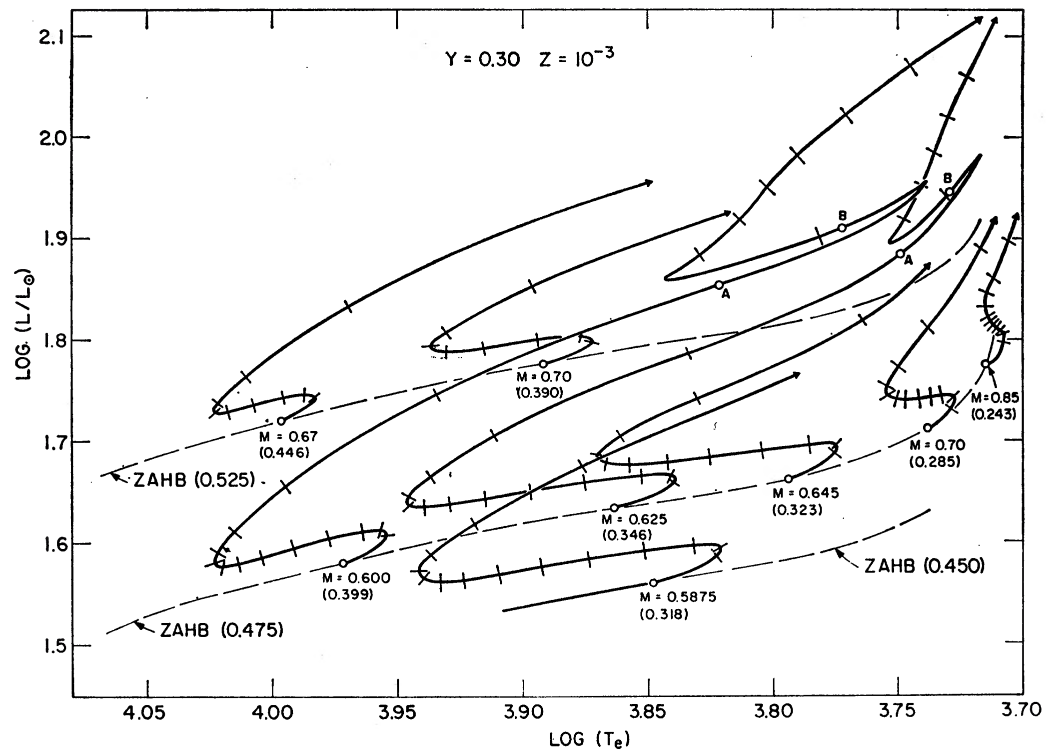

a

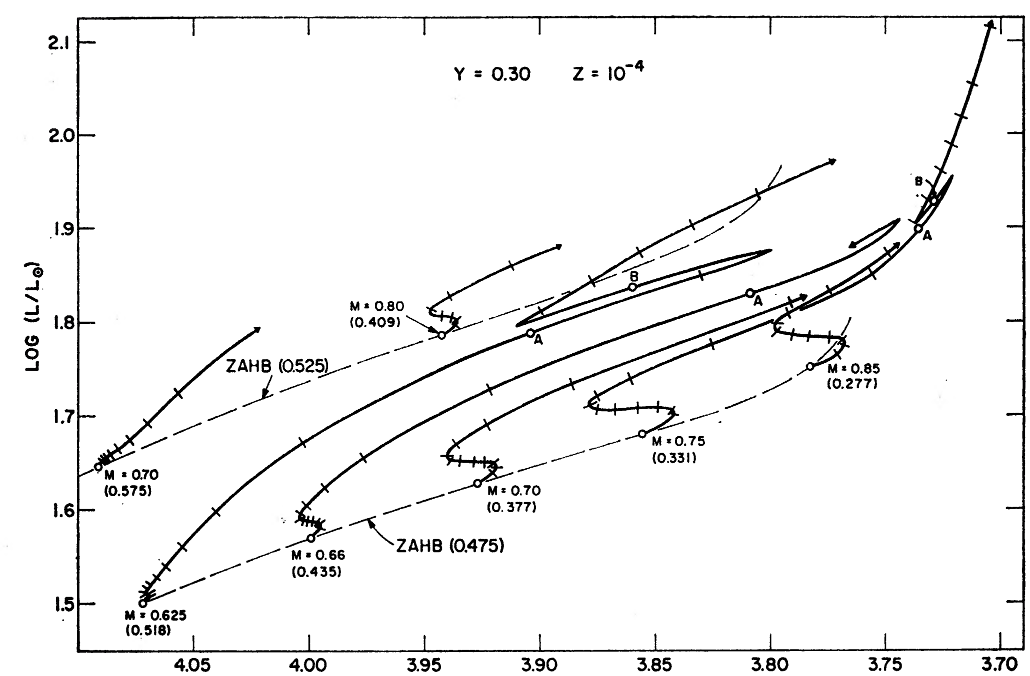

b

FIG. 1.—Evolutionary tracks during core helium burning. Composition choices are: (*a*) $Y = 0.3$, $Z = 10^{-3}$; (*b*) $Y = 0.3$, $Z = 10^{-4}$; (*c*) $Y = 0.2$, $Z = 10^{-3}$ and 10^{-4}; (*d*) $Y = 0.1$, $Z = 10^{-3}$ and 10^{-4}. The separation between two adjacent tick marks along each evolutionary track corresponds to an interval of 5×10^6 yr. Each dashed line labeled ZAHB defines the locus of starting models of the same initial core mass (given in parentheses in units of $M_\odot$). The total mass M of each evolved model is given in units of $M_\odot$. In parentheses below each mass designation in Fig. 1, *a* and *b*, is the fraction of the total luminosity of the initial model that is produced in the helium core. Four models for $Y = 0.3$ are carried beyond the phase of core helium burning. Points *A* indicate where the central helium $Y_C = 0.01$. At point *B* the convective core vanishes.

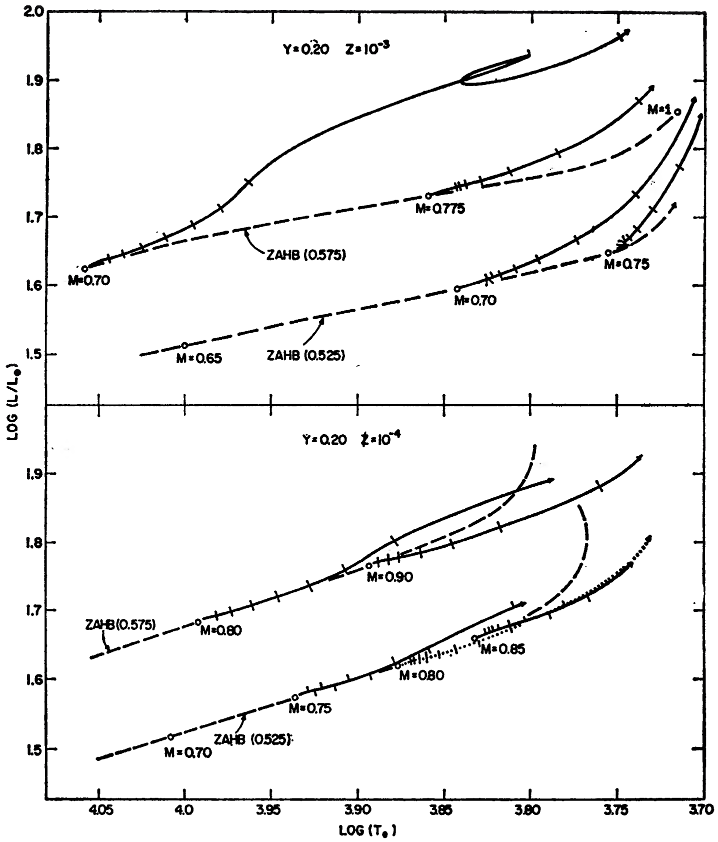

c

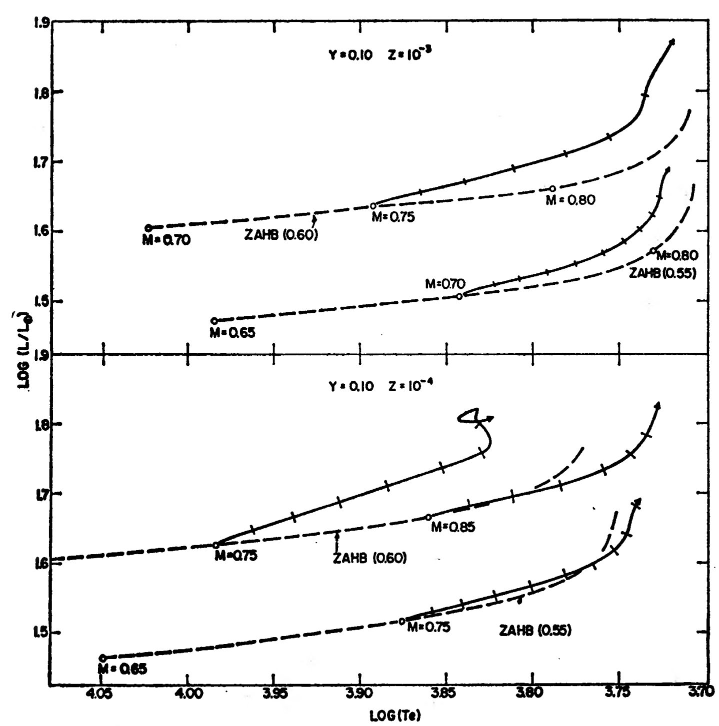

d

FIG. 1.—*Continued*

branch lifetime" as a function of all parameters. There is, of course, some ambiguity in deciding at what point a model ceases to be on the horizontal branch. We shall here *define* horizontal-branch lifetime t_{HB} as the time required for the central helium abundance to be reduced to $Y_C = 0.01$. Lifetime so defined is given in Table 1 and in Figure 2 as a function of the pertinent parameters. Since, for a fixed core mass, lifetime is not insensitive to variations in Z and M, the properties of the core are coupled to the properties of the envelope much more strongly than might have been anticipated.

The horizontal-branch lifetimes quoted here are somewhat larger (by about 20 percent when $Y = 0.3$ and by about 10 percent when $Y = 0.2$) than those quoted by Iben and Rood (1969). The discrepancy is due to a difference in the definition of t_{HB}. Our earlier estimates were based on a judgment that the last and most luminous portion of an individual track during core helium burning might correspond not to stars normally assigned to the horizontal branch in real clusters, but rather to stars near the base of a secondary giant branch. The fact that models of double shell sources evolve on a long time scale along tracks that define a secondary giant branch suggests that the earlier assumption was inappropriate.

In Table 1 and in Figure 2 are compared the value of t_{HB} as derived from evolutionary calculations with the lifetime $(t_{HB})_0$ estimated in Paper II on the assumption that core luminosity and the mass M_{CC} in the convective core remain fixed at their initial values. In no case do estimated and computed lifetimes differ by more than 20 percent. The good agreement demonstrates that, indeed, L_{He} and M_{CC} are relatively constant during evolution.

There is an uncertainty in t_{HB} due to an uncertainty in the effective–cross-section factor for the $^{12}C(\alpha,\gamma)^{16}O$ reaction. We have assumed, on the strength of calculations by Stephensen (1966), that the reduced width for the reaction is $\theta_\alpha^2 = 0.078$, or about 10 times lower than the theoretical maximum of 1. With this choice of θ_α^2, there are roughly equal numbers of ^{12}C and ^{16}O left after helium is exhausted at the center. Had we chosen $\theta_\alpha^2 > 0.78$, ^{16}O would have been by far the dominant end product of core helium burning. Since we have no assurance that the assumptions that lead to $\theta_\alpha^2 \sim 0.1$ are met in nature, it is important to know the sensitivity of t_{HB} to the choice of θ_α^2.

Since M_{CC} and L_{He} are to good approximation constant during evolution, $t_{HB} \sim M_{CC}E/L_{He} \sim \text{const.} \times E$, where E is the total energy released per gram in the convective core. We may write $E(\text{ergs}) = 1.167 \times 10^{-5}(N_{12} + N_{16}) + 1.145 \times 10^{-5}\ N_{16}$, where N_{12} and N_{16} are, respectively, the number of ^{12}C and ^{16}O nuclei in 1 g at the end of core helium burning. Since $N_{12} \tilde{\propto} X_{12}/12$ and $N_{16} \tilde{\propto} X_{16}/16$, where X_{12} and X_{16} are the abundances by mass of ^{12}C and ^{16}O in the final mix, number conservation gives $X_{12}/12 + X_{16}/16 = \frac{1}{4}$. Thus $t_{HB} \propto (1 + 0.246\ X_{16})$. If, then, θ_α^2 lies between 0.08 and 0.8 so that X_{16} lies between about $\frac{1}{2}$ and 1 in the final mix, t_{HB} is uncertain by roughly 10 percent. The values in Table 1 and Figure 2 are on the lower edge of the range; that is, they correspond to the case $\theta_\alpha^2 \sim 0.1$ or $X_{16} \sim \frac{1}{2}$ in the final mix. Our estimate of the uncertainty in t_{HB} agrees with that found by Iben and Faulkner (1968) as a result of explicit evolutionary calculations.

c) Models with Two Shell Sources and an Asymptotic Branch

We have evolved four models for $Y = 0.3$ and initial core mass $M_C = 0.475\ M_\odot$ somewhat beyond the phase of helium exhaustion in the core. The evolutionary tracks for these models are shown in Figure 1, *a* ($M = 0.600\ M_\odot$ and $M = 0.625\ M_\odot$) and *b* ($M = 0.625\ M_\odot$ and $M = 0.75\ M_\odot$). The points on the tracks where $Y_C = 0.01$ are marked A. The surface temperature starts to increase when the size of the convective core begins to decrease; the convective core vanishes rapidly and is completely gone at the point marked B. In the $Z = 10^{-3}$ cases, $Y_C \to 0$ at a luminosity that is about 0.4 mag brighter than the ZAHB.

The period of evolution to the blue is very brief. During most of the double-shell-

TABLE 1

HORIZONTAL-BRANCH LIFETIMES ($Y_C = 0.01$)

$M_C/M_\odot$	$M/M_\odot$	Y	$-\log Z$	$t_{HB}/10^7$ yr	$t_{HB}/(t_{HB})_0$	L_{He}/L
0.450	0.588	0.3	3	7.57	0.87	0.318
0.475	0.85	...	...	6.04	0.84	0.243
...	...	...	...	5.95	0.88	0.277
...	0.75	...	...	6.20	0.93	0.331
...	0.70	...	3	6.25	0.87	0.285
...	...	...	4	6.15	0.92	0.377
...	0.66	...	...	6.40	0.96	0.435
...	0.645	...	3	6.33	0.89	0.323
...	0.625	...	3	6.80	0.97	0.394
...	...	...	4	6.39	0.97	0.530
...	0.60	...	3	6.80	0.97	0.396
0.525	0.80	...	4	4.64	0.99	0.409
...	0.70	...	3	4.49	0.91	0.390
...	...	...	4	4.76	1.03	0.574
...	0.67	...	3	4.90	1.00	0.446
...	0.85	0.2	4	4.67	1.00	0.552
...	0.80	...	4	5.02	1.08	0.604
...	0.75	...	3	4.76	0.98	0.533
...	...	...	4	4.83	1.03	0.672
0.550	0.75	0.1	3	4.90	1.14	0.890
...	0.70	...	4	4.49	1.07	0.882
0.575	0.90	0.2	4	3.65	1.02	0.633
...	0.80	...	...	3.75	1.04	0.761
...	0.775	...	3	3.70	0.98	0.641
...	0.70	...	...	3.70	1.04	0.822
0.600	0.85	0.1	4	3.48	1.06	0.903
...	0.75	...	3	3.69	1.09	0.927
...	...	...	4	3.54	1.06	0.957

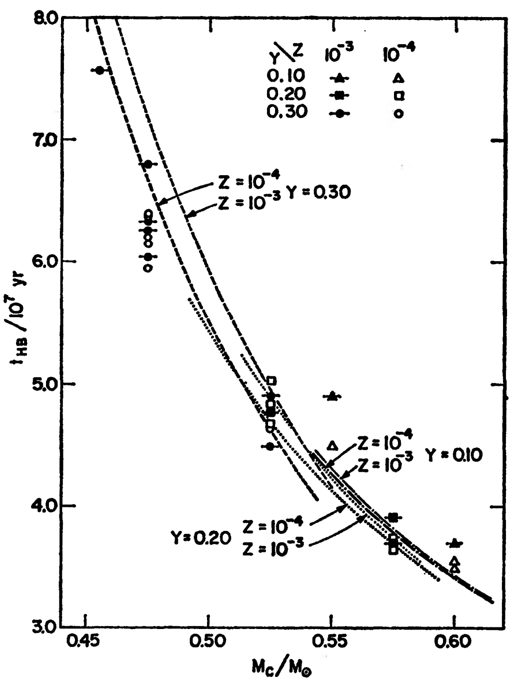

FIG. 2.—Horizontal-branch lifetime as a function of assumed core mass and composition. *Triangles*, *squares*, and *circles*, results of evolutionary calculations. *Dash*, *dot*, and *dash-dot curves*, results of an extrapolation based solely on the properties of initial horizontal-branch models.

source phase, models evolve upward and to the red along a secondary giant branch that, for the models shown, approaches the giant branch defined by models burning hydrogen in a shell.

As each double-shell-source model mounts upward along its secondary or "asymptotic" giant branch, the helium-burning shell approaches the hydrogen-burning shell more closely. We have evolved models only until the mass between the center and the helium-burning shell reaches from one-half to two-thirds of the mass between the center and the hydrogen-burning shell. Extrapolating from the available information, we can estimate the time which elapses between the end of core helium burning and the point when the helium shell nearly reaches the hydrogen shell for the first time. We tentatively call this time t_{AB}, the lifetime along the asymptotic branch. Our estimates for t_{AB} are given in Table 2, together with the actual time Δt_{AB} for which we have evolved the double-shell-source models.

Our estimates show that t_{AB} is comparable to t_{HB} and that therefore the asymptotic branch in real clusters should be (within a factor of 2, at least) nearly as well populated as the horizontal branch. We defer a quantitative comparison with the observations until Papers IV and V, after we have constructed a more complete set of asymptotic-branch models and have obtained better estimates of t_{AB}.

TABLE 2

ESTIMATES OF ASYMPTOTIC-BRANCH LIFETIMES (10^7 years)

$M/M_\odot$	$-\log Z$	t_{HB}	Δt_{AB}	$\sim t_{AB}$	$\sim t_{AB}/t_{HB}$
0.625.......	3	6.8	3.84	4.4	0.65
0.600.......	...	6.8	3.58	4.9	0.71
0.750.......	4	6.2	3.20	4.5	0.72
0.625.......	...	6.4	2.90	5.3	0.83

IV. THE TIME DEPENDENCE OF STRUCTURE VARIABLES IN A $Y = 0.3$ MODEL

We suggest that those more interested in comparing surface features with the observations than in appreciating the interplay between interior occurrences and surface changes turn immediately to § V.

In Figure 3, *a–f*, is shown the time dependence of several significant interior and surface quantities describing the model with $M = 0.625\ M_\odot$, $M_C = 0.475\ M_\odot$, $Y = 0.30$, and $Z = 10^{-3}$. Most quantities in these figures require no explanation. The center of the helium-burning shell is defined as the point interior to which half of the total helium-burning luminosity L_{He} is produced. Quantities describing this point are thus well defined even when helium is burning at the center. The center of the hydrogen-burning shell is defined as the point interior to which half of the total hydrogen luminosity L_H is produced. Eighty percent of the energy output due to helium burning occurs in a region of mass ΔM_{He}, and 80 percent of that due to hydrogen burning occurs in a region of mass ΔM_H. If it is assumed that the period at which the model will pulsate in the fundamental mode is proportional to the $\frac{3}{2}$ power of the radius, the quantity $1.5\ R^{-1}\ dR/dt$ in Figure 3, *a*, represents the fractional rate of period change.

The evolutionary behavior of a horizontal-branch model with high envelope helium involves a complex interplay of competing processes. We shall attempt to describe these processes without pretending to explain them.

In the initial model, the convective region at the center of the helium core contains a mass of $0.11\ M_\odot$. During evolution, the convective region grows slowly in mass until helium is essentially exhausted at the center. As shown by the position and size of the helium "shell" in Figure 3, *e*, helium burning is concentrated in a small central portion

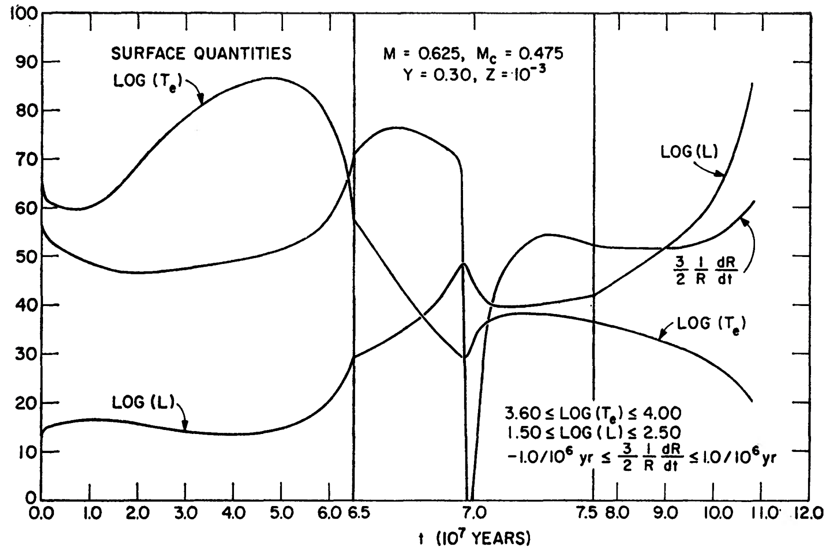

a

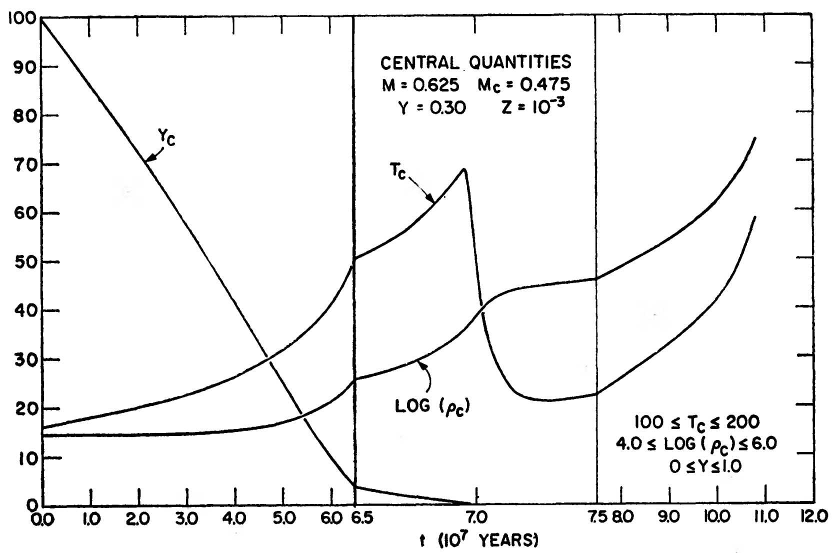

b

FIG. 3.—Time dependence of interior and surface characteristics for the case $Y = 0.3$, $Z = 10^{-3}$, $M = 0.625\ M_\odot$, and initial $M_C = 0.475\ M_\odot$. Characteristics shown are: (*a*) effective temperature T_e, luminosity L, and rate of period change $3dR/2Rdt$ per 10^6 years; (*b*) central density ρ_C, central temperature T_C, and central helium abundance Y_C; (*c*) helium-shell-burning quantities: density ρ_{sh}, temperature T_{sh}, and radius R_{sh}; (*d*) hydrogen-shell-burning quantities: density ρ_{sh}, temperature T_{sh}, and radius R_{sh}; (*e*) location (M_H, M_{He}) and size (ΔM_H, ΔM_{He}) of the hydrogen- and helium-burning shells, respectively; (*f*) total luminosity L and its components: helium-burning luminosity L_{He}, total hydrogen-burning luminosity L_H, and CN-cycle luminosity L_{CN}. All central and shell temperatures and densities are given in units of 10^6 ° K and g cm^{-3}, respectively. Luminosities, radii, and masses are all in solar units. Scale limits are described in each figure.

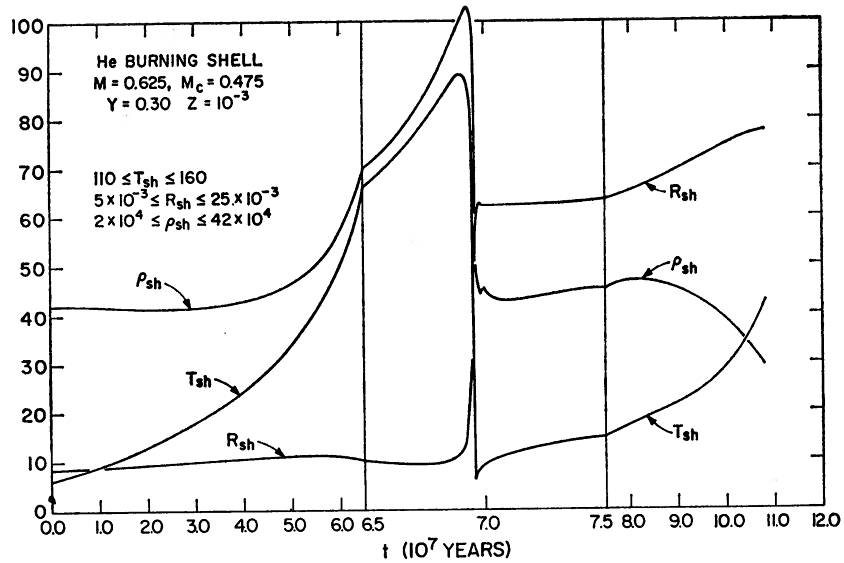

c

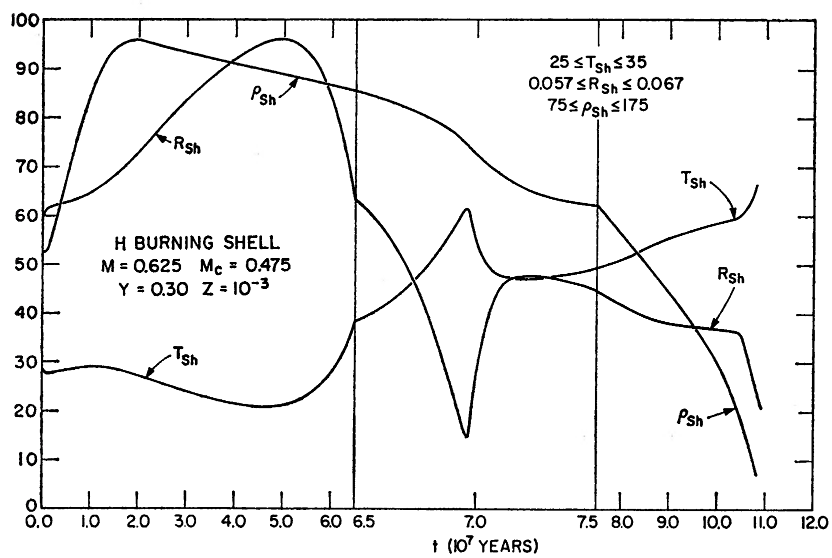

d

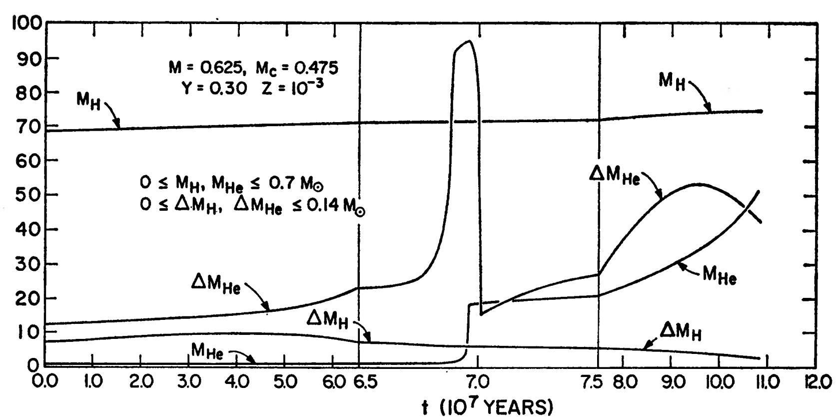

e

FIG. 3.—*Continued*

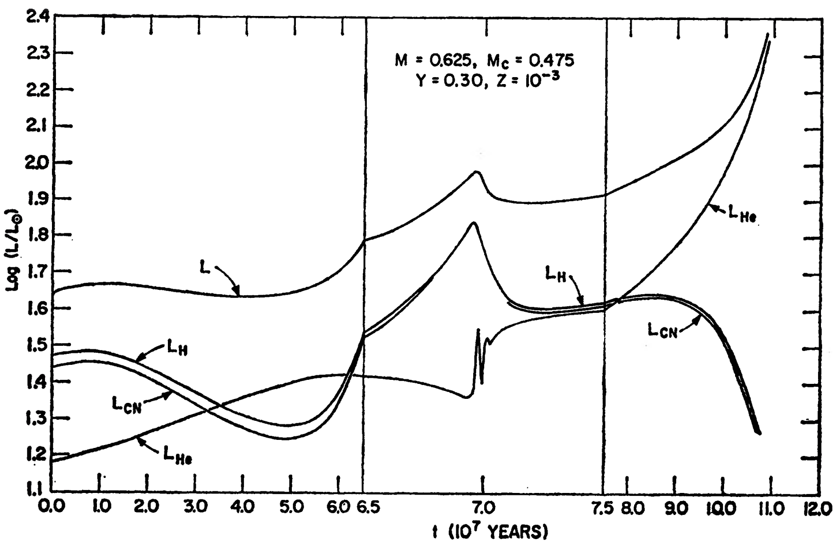

f

FIG. 3.—*Continued*

of the convective region. As helium is converted into carbon and thence into oxygen, the molecular weight of the entire convective region rises uniformly. Pressure balance is maintained primarily by an increase in central and shell temperatures; densities in the convective region remain essentially constant. As a result of rising interior temperatures, L_{He} increases. Another factor contributing to the rise in helium-core temperatures and in L_{He} is the fact that the hydrogen-burning shell continues to add mass to the core. To simplify the discussion we will continue to refer to the entire region within the hydrogen-burning shell as the helium core, even after considerable quantities of carbon and oxygen have been formed.

As L_{He} increases, the outer regions of the helium core expand. The tendency toward outward motion extends into the base of the hydrogen-burning shell where temperatures drop. The concomitant decrease in L_{H} almost exactly compensates for the increase in L_{He}, and the total luminosity remains nearly constant during much of the horizontal-branch phase.

The increase in molecular weight within the hydrogen-burning shell engenders a tendency for contraction to occur in the vicinity of the shell. As shown in Figure 3, *d*, shell densities actually rise for a time even though the center of the shell continues to move outward into fresh unburned material at larger distances from the origin. After the short initial excursion to the red in the H-R diagram (part of which is due to an adjustment of composition variables in the hydrogen shell from an initially imposed distribution to the correct one), the entire region between the base of the hydrogen-burning shell and the stellar surface contracts and the star evolves to the blue.

We remark parenthetically that in models with relatively weak hydrogen-shell sources (e.g., models with a much lower helium abundance in the envelope), the molecular weight near the shell does not increase rapidly enough to offset the core-induced tendency for expansion. For such models, evolution proceeds continuously to the red in the H-R diagram until helium is exhausted at the center.

When the central helium abundance drops to about 0.3 in the high-Y model under consideration, evolutionary changes undergo a radical revision. The entire helium core contracts, the hydrogen-burning shell moves inward toward the center, and the envelope (beginning in a region slightly beyond the outer edge of the shell) expands outward. The star evolves to the red in the H-R diagram and brightens.

One may attribute this change in behavior to the fact that energy production by helium burning is proportional to a rather high power (the cube) of the helium abundance. Once Y_C^3 drops below some critical value (in this case, $Y_C^3 \lesssim 0.027$), an increase in core temperatures alone is not sufficient to maintain a flux balance; core densities must also increase.

The expansion of the envelope may be correlated with an increase in the rate at which the total stellar luminosity increases. As the helium core contracts and heats, $L_{\rm He}$ continues to rise. Matter in the hydrogen-burning shell is drawn inward to higher temperatures, and $L_{\rm H}$ also increases. The situation is analogous to that in massive main-sequence stars: the entire region involved in energy production moves inward and heats, while the outer, inert portions of the star move outward to accommodate the increasing rate of energy production.

The interior structure when the model is near the point when redward motion in the H-R diagram supersedes blueward motion is shown in Figure 4, *a*. The composition discontinuities near a mass fraction of 0.2 are due to the fact that the mass of the convective region has grown continuously. The variation of the luminosity variable shows that helium burning is still concentrated very near the center. Hydrogen burning accounts for about 40 percent of the total surface luminosity.

As evolution continues, the central helium abundance eventually becomes so small that $L_{\rm He}$ begins to drop even though core temperatures and densities continue to rise. However, temperatures in the hydrogen-burning shell continue to rise sufficiently rapidly that the decrease in $L_{\rm He}$ is more than offset by an increase in $L_{\rm H}$ and the model continues to evolve to the red in the H-R diagram.

The more nearly Y_C^3 approaches zero, the more rapidly do structural changes occur. It is for this reason that we have introduced the expanded scale in Figure 3 between $t = 6.5 \times 10^7$ yr and 7.5×10^7 yr ($t_7 = 6.5$–7.5).

During the period $t_7 \sim 6.8$ to $t_7 \sim 7.0$, the region of maximum energy production by helium burning shifts from near the center to a shell. As this occurs, the quantity $\Delta M_{\rm He}$ in Figure 3, *e*, is not a true measure of the mass actively involved in strong helium burning. This is because there is a large region of relative inactivity that separates the peak of the dying core source from the peak of the developing shell source. The quantity $\Delta M_{\rm He}$ remains anomalously large until the contribution of the residual core source to $L_{\rm He}$ drops below 10 percent at $t_7 \sim 7.0$.

After reaching a maximum of $0.125\ M_\odot$ at $t_7 = 6.95$, the mass in the convective region drops extremely rapidly, and central convection disappears by $t_7 = 6.99$. The subsequent evolution of the "helium" core is analogous to the evolution of a middle-main-sequence star following the disappearance of the central convective region and the exhaustion of central hydrogen. The central temperature drops rather abruptly, but temperatures in the newly formed shell rise until the pure carbon-oxygen core becomes nearly isothermal. Helium burning in the shell is "explosive" in the sense that it overheats and forces matter ahead of it to expand and cool.

As a consequence of the expansion induced by the helium shell, the hydrogen-burning shell is pushed out to larger radii and lower temperatures. At first $L_{\rm H}$ decreases more rapidly than $L_{\rm He}$ increases. In response to the decrease in total luminosity, the stellar envelope contracts. The model dims and evolves to the blue in the H-R diagram.

Eventually the increase in $L_{\rm He}$ overshadows the decrease in $L_{\rm H}$ and the model star reverses direction in the H-R diagram, evolving upward and to the red on a time scale comparable to the duration of the phase of core helium burning.

The interior of one of the last models computed is shown in Figure 4, *b*. Notice how shallow the temperature gradient is in the carbon-oxygen core. Notice also how minor the contribution of $L_{\rm H}$ is to the total surface luminosity. What this means is that the model star behaves essentially like a model of a single shell source, of which a hydrogen-burning red giant is the prototype. The comparison is even more apt than this, since electron degeneracy becomes appreciable at the center of the stars burning helium in a shell. At the center of the model shown in Figure 4, *b*, electron degeneracy contributes half of the total pressure.

Neutrino losses by pair annihilation, the plasma process, and the photoneutrino process have been neglected in all of the helium-burning phases we have described. Energy loss by plasma neutrinos, if it occurs, may be expected to have a significant effect on the

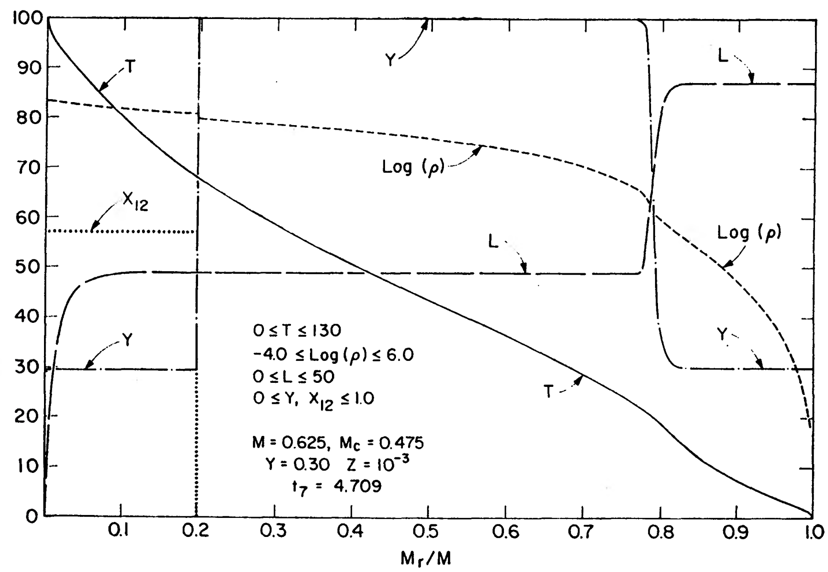

a

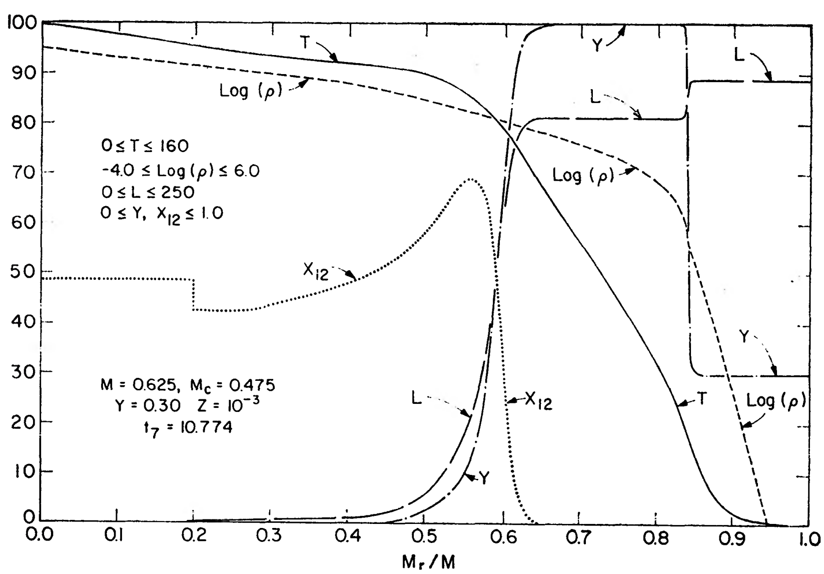

b

FIG. 4.—Internal structure (*a*) during the phase of core helium burning and (*b*) during the double-shell-source phase for the case $Y = 0.3$, $Z = 10^{-3}$, $M = 0.625\ M_\odot$, $M_C = 0.475\ M_\odot$. Symbols have the following meaning: T = temperature (10^6 ° K); ρ = density (g cm^{-3}); L = luminosity ($L_\odot$); Y = helium abundance by mass; X_{12} = carbon abundance by mass; M_r/M = mass fraction. Scales are shown in the figures.

structure of the carbon-oxygen core during the latter stages of asymptotic-branch evolution. In the model depicted in Figure 4, *b*, the rate of energy loss by the plasma process, if it occurs, is on the order of 2 $L_{\odot}$, or roughly 1 percent of the nuclear luminosity.

V. IS THERE A SPREAD IN STELLAR MASS ALONG THE HORIZONTAL BRANCH?

a) Mismatch between Observation and Theory with No Mass Spread

In several extremely metal-poor globular clusters, the horizontal branch extends between approximately 0.4 and -0.1 in $B - V$ (after approximate corrections for reddening have been made). This corresponds roughly to the range 3.8–4.1 in log T_e. In several clusters that are less metal-deficient, the color limits of the horizontal branch lie considerably beyond 0.4 to -0.1 in $B - V$. Using selected observational data (Searle and Rodgers 1966; Sandage 1969; Newell, Rodgers, and Searle 1969; Newell 1970) in conjunction with the properties of theoretical model atmospheres, Newell (1970) estimates the following widths in log T_e: 3.80–4.10 (ω Cen); 3.85–4.13 (M92); 3.85–4.10 (NGC 6637); 3.76–4.15 (M3); 3.88–4.28 (M13). Although these limits on log T_e are based on a transformation from $B - V$ that cannot be said to be firmly established, it is perhaps safe to conclude that stellar-structure theory must in several instances account for a horizontal-branch width of at least 0.3 in log T_e.

Previous attempts at describing the horizontal branch by means of theoretical models have assumed that all stars on the branch have essentially the same mass and that each star traverses the entire width of the branch during its sojourn there. To be sure, several published tracks (e.g., Faulkner and Iben 1966; Hartwick, Härm, and Schwarzschild 1968) actually extend over a range $\Delta(\log T_e) \sim 0.3$, showing that, by an appropriate (not necessarily correct) choice of input parameters and input physics, it is possible to match with the track of a single model the color widths attributed to some of the horizontal branches appearing in nature.

However, horizontal-branch width is not the only cluster characteristic that must be accounted for by stellar-structure theory. There are several observationally and theoretically well-defined relationships between properties of horizontal-branch stars and stars evolving between the main sequence and the red-giant tip that impose constraints on the possible range of input parameters for horizontal-branch models. Using the best available input physics and choosing parameters in such a way as to satisfy these constraints, evolutionary paths during core helium burning are disappointingly short compared to horizontal-branch widths estimated from the observations. The tracks in Figure 1 are good examples.

b) The Limitation on the Range of Input Parameters

If the helium flash is a well-behaved phenomenon that proceeds after the manner given by quasi-static calculations of spherically symmetric models, then the mass in the helium core of a star as it first arrives on the horizontal branch is a well-behaved function of initial composition that can in principle be determined properly (by giant-branch calculations) if the proper opacities, etc., have been chosen. In the most comprehensive exploration to date, Eggleton (1968) has estimated the dependence on composition of the maximum core mass at the red-giant tip. For example, interpolation in his results for the case $Y = 0.30$ and $Z = 10^{-3}$ gives $M_C \simeq 0.44\ M_{\odot}$ if neutrino losses by the plasma process are neglected ($\epsilon_{\nu\nu} = 0$) and $M_C \simeq 0.48\ M_{\odot}$ if these neutrino losses are included ($\epsilon_{\nu\nu} = 0$). For the case $Y = 0.30$, $Z = 10^{-4}$, Eggleton's results give $M_C \simeq 0.46\ M_{\odot}$ if $\epsilon_{\nu\nu} = 0$ and $M_C \simeq 0.50\ M_{\odot}$ if $\epsilon_{\nu\nu} \neq 0$.

Once the initial mass of the helium core has been determined, the relationship between absolute luminosity and surface temperature along the appropriate theoretical horizontal branch is established. In particular, the absolute luminosity L_{RR} of an average RR Lyrae star has been established. Note from Figure 1 that, for most of a star's core-helium-burning lifetime, the evolutionary path remains sufficiently close to the ZAHB that the relationship between L and T_e can be estimated in first approximation simply by constructing the ZAHB.

The lifetime of a theoretical horizontal-branch model is approximately a function only of the initial mass of the helium core. Core mass at the time of the helium flash is nearly independent of total stellar mass and is consequently nearly independent of cluster age and of the extent of mass loss along the giant branch. One can therefore define a mean horizontal-branch lifetime t_{HB} that is primarily a function of initial composition and write $t_{\mathrm{HB}} = t_{\mathrm{HB}}(Y, Z)$. One can also define a red-giant lifetime $t_{\mathrm{RG}}(L_{\mathrm{RG}}, Y, Z)$ as the time required by a giant-branch star to evolve toward the red-giant tip beyond a luminosity L_{RG}. Since the mean luminosity L_{RR} of a theoretical RR Lyrae variable has been determined as a function of Y and Z, it is convenient to choose $L_{\mathrm{RG}} \simeq L_{\mathrm{RR}}$. With this convention, one may construct $t_{\mathrm{HB}}/t_{\mathrm{RG}}$ as a function of Y and Z.

From the observations for any cluster one can in principle determine the quantities N_{HB} (=the number of stars on the horizontal branch) and N_{RG} (= the number of stars along the giant branch beyond the luminosity level of RR Lyrae stars in the cluster). Equating $N_{\mathrm{HB}}/N_{\mathrm{RG}}$ to $t_{\mathrm{HB}}/t_{\mathrm{RG}}$ then establishes a relationship between Z and Y. If, finally, Z can be estimated from spectroscopic data, a value of Y can be assigned to stars in a given cluster.

Proceeding in this way (Iben 1968; Iben and Rood 1969; Iben *et al.* 1969), one finds that if $Z = 10^{-3}$–10^{-4}, then $Y \sim 0.3$ (± 0.05) describes stars in those metal-poor clusters for which sufficient observational data exist. Using the values of t_{HB} given in § III alters this to $Y \sim 0.29 \pm 0.05$. The spread in estimated Y is in part a measure of the uncertainty in the initial mass of the helium core and of the uncertainty in t_{HB} and t_{RG}. A full account of the procedure and the uncertainties will be given in Paper V of this series.

c) *Estimates of the Mass Spread in M3*

Having estimated the composition and initial core mass of horizontal-branch stars in any given cluster, one can estimate the extent of the mass spread necessary to account for the observed width of the horizontal branch in that cluster. We shall select the cluster M3 for comparison with models and assume that Newell's (1970) estimate of $\Delta(\log T_e) \sim 0.4$ for the width of the horizontal branch is roughly correct. We assume finally that models constructed with the parameter set $Y = 0.30$, $Z = 10^{-3}$, $M_C = 0.475\ M_\odot$ are roughly appropriate.

Inspection of Figure 1, *a*, reaffirms that no single evolutionary track covers (on a long time scale) a range that is even remotely close to the range estimated from the observations. If one accepts quite literally the interpretation that $\log T_e \sim 3.76$–4.15 for the horizontal branch in M3 and if one accepts with equal confidence our choices for composition and core mass, it follows that the mass of a star near the blue end of the horizontal branch is approximately $0.56\ M_\odot$ whereas the mass of a star near the red end is approximately $0.76\ M_\odot$. Since our choice of composition, particularly of Z, can at best be only a rough approximation and since the limits in $\log T_e$ are only rough estimates, it is perhaps wise to avoid emphasis on absolute values. If one retains the assumption that $\Delta(\log T_e) \sim 0.4$ but allows the low-temperature edge to be uncertain by perhaps 0.03 in $\log T_e$, it follows that the total variation in mass along the horizontal branch in M3 could be on the order of 0.1–$0.2\ M_\odot$.

One might go so far as to attempt to derive what the distribution in number versus mass on the M3 horizontal branch actually is. A realistic analysis of the actual situation would be premature and should be avoided until we have (1) a much finer grid of horizontal-branch models; (2) an appreciation of the sensitivity of model surface temperature to l/H; (3) a more firmly established relationship between $B - V$ and $\log T_e$; and (4) a complete sample of horizontal-branch stars not biased by selection. We shall instead present a qualitative illustration of the type of information one might obtain from an analysis of the mass distribution.

Let us suppose that the distribution in number N versus $B - V$ is flat so that $dN/d(B - V) = 0$. Our first task is to convert this distribution into one which relates number N to $\log T_e$. To accomplish this we require a relationship between $B - V$ and $\log T_e$ from which we can derive $d(B - V)/d(\log T_e)$. Since $dN/d(B - V) = 0$, we have $N(\log T_e) \propto -d(B - V)/d(\log T_e)$. The choice of $d(B - V)/d(\log T_e)$ that we show in Figure 5, although purposefully somewhat arbitrary, exhibits qualitatively correct features: a shallow slope at the extreme edges of the temperature range and a much steeper slope at intermediate temperatures. What it says is that, if the horizontal branch is evenly populated in the color coordinate $B - V$, then, in the theoretical coordinate $\log T_e$, the red portions of the horizontal branch are much more heavily populated than the blue portions.

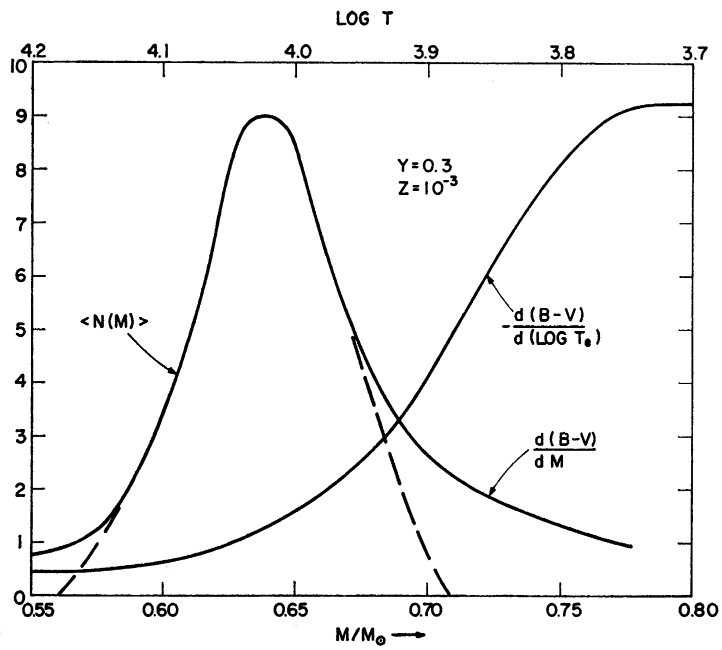

FIG. 5.—An illustrative estimate of the distribution versus mass $N(M)$ of stars along the horizontal branch of a hypothetical cluster. It is assumed that stars are distributed uniformly in $B - V$ and that the relationship between $B - V$ and $\log T_e$ has the slope shown in the figure. The relationship between M and $\log T_e$ is that appropriate to the theoretical case for $Y = 0.3$, $Z = 10^{-3}$ discussed in the text. The dashed curve is appropriate if $N(B - V)$ falls to zero at either end of an otherwise constant distribution. The normalization of all curves is arbitrary.

The next step in our illustrative analysis requires a knowledge of the relationship between M and $\log T_e$ for horizontal-branch models. Again we choose the parameters $Z = 10^{-3}$, $Y = 0.3$, and $M_C = 0.475\ M_\odot$ and plot in Figure 6 the relationship between mass and surface temperature for each of three locations on the evolutionary tracks: (1) the ZAHB; (2) the maximum redward extent before turning to the blue; (3) the maximum blueward extent before turning back to the red. Over 80 percent of the lifetime of a core-helium-burning model is spent between the temperature limits corresponding to points 2 and 3. To derive an approximate N versus M distribution, we first assume that a model of any mass remains at location 2 during its entire lifetime; we then multiply each point along the $N(\log T_e)$ curve in Figure 5 by the appropriate value of $d \log T_e/dM$ derived from curve 2 in Figure 6. This gives a distribution $N_2(M)$. We next assume that a model spends its entire life at location 3 and construct the curve $N_3(M)$. Averaging $N_2(M)$ and $N_3(M)$ gives the final approximation to $\langle N(M)\rangle$ shown in Figure 5.

If we were to impose limits on the N versus $B - V$ distribution so that $N(B - V)$

drops smoothly to zero at either end of a flat distribution, we would obtain a modified N versus M distribution similar to that defined by the dashed lines in Figure 5.

We emphasize once again that our example is entirely illustrative. The occurrence of a peak in the distribution is in part due to the fact that the curves $M(\log T_e)$ in Figure 6 depart from linearity at low surface temperatures where envelope convection becomes important. We could have cut off the N versus $B - V$ distribution at a value such that the cutoff value of log T_e was still on the linear portion of the curve M versus log T_e; we could have adjusted Z and Y or the ratio l/H of mixing length to scale height in such a way as to move the nonlinear portion of the ZAHB beyond the surface temperature at which we cut off the initial distribution. Had we performed either of these operations, then the maximum in $N(M)$ might have occurred at the cutoff value for M. Much more exploration with theoretical model interiors and a better understanding of the transformation of $B - V$ to log T_e should be a prerequisite for any serious analysis of

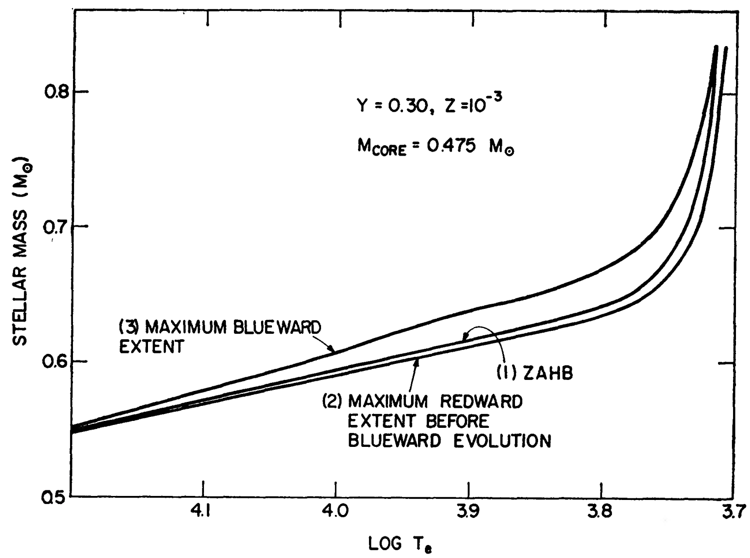

FIG. 6.—Relationship between stellar mass and log T_e for the case $Y = 0.3$, $Z = 10^{-3}$, $M_C = 0.475$ $M_\odot$. Each curve represents the locus of corresponding points along the appropriate evolutionary tracks in Fig. 1, *a*.

the mass distribution along the horizontal branch of any real cluster. Equally important is the availability of a complete N versus $B - V$ distribution that does not suffer from observational selection.

d) A Mass Variation in the Opposite Sense?

Woolf (1964) has shown that when horizontal-branch stars in M3 are grouped according to color, there are differences in the space distributions defined by members of each group. Blue stars define a somewhat more centrally condensed distribution than do yellow stars; yellow stars in turn define a somewhat more centrally condensed distribution than do red ones.

Assuming that the differences are statistically significant and that stars in each group define a relaxed distribution in the sense of equilibrium statistical mechanics, Woolf argues that the average blue star is more massive than the average yellow star and that the average yellow star is in turn more massive than the average red one.

This order is, of course, exactly opposite to the one which we have suggested. We remark that the 5×10^7 years that a star remains on the horizontal branch may be insufficient for relaxation to be achieved and/or that the apparent correlation between color and space distribution may not be statistically significant.

e) *Is There a Spread in Z?*

Another way of increasing the width of a theoretical horizontal branch is to assume that there is an appreciable variation in appropriate Z-values and perhaps also in the CNO/metals ratio from one star to another in a given cluster. It is not difficult to understand how a large variation might arise.

Any defense of the popular hypothesis that stars in globular clusters are among the last remaining members of the first generation of stars to form (possibly after the emergence of pregalactic matter from a fireball state) must explain why the metal abundance at the surfaces of cluster stars appears to be several orders of magnitude larger than that produced in either a big bang or in possible, subsequent "little bangs" (Wagoner, Fowler, and Hoyle 1967). If the heavy elements in the globular clusters were not of fireball or of little-bang origin, where then did they originate? Peebles and Dicke (1968) suggest that the heavy elements are a result of contamination by an internal supernova that presumably exploded prior to the formation of the majority of cluster stars. Another possibility is that prestellar matter in protoclusters was contaminated by debris blown out from massive stars that formed near the galactic center toward the end of a postulated galactic collapse.

The first suggestion (internal supernova) has difficulty in accounting simply for the apparent correlation between metal deficiency and average distance from the galactic center (Eggen, Lynden-Bell, and Sandage 1962) that appears to hold for halo stars in the field. The correlation may be presumed to hold also for globular clusters, particularly if most halo stars were once members of globular clusters that have been stripped and finally destroyed by multiple encounters with each other. The second suggestion (external contamination) explains the correlation by supposing that the most metal-deficient clusters were farthest away from the galactic center during the most active period of heavy-element production near the center. Since they reached the disk only after most of the contaminants there had been locked away into low-mass stars that are still in existence today, these clusters experienced less contamination.

The particular mode of contamination is not of importance for our argument. It is the necessity of having to invoke a contaminating process that is of major relevance. Whether prestellar matter in protoclusters was contaminated from the inside or from the outside, the extent of contamination should show a variation with position in the cluster—e.g., matter farther from the internal source should contain a lower abundance of heavy elements than matter closer to the source.

A variation in Z and/or in Z_{CNO}/Z among stars of a given cluster would certainly account for some of the spread in observed horizontal branches. It would also suggest that clusters may differ as to the mode of initial contamination and thereby offer some help in interpreting the "anomalies" that appear in any attempt to correlate the appearance of cluster diagrams with some metallicity indicator.

The possibility of a significant spread in Z or Z_{CNO} could of course be easily tested if several widely separated cluster stars of similar color and magnitude were subjected to complete spectrum scans and model-atmosphere analysis.

VI. M3 AND HIGH-Z MODELS

An attempt to provide a general accounting of the properties of all metal-poor clusters will be presented in Paper IV. In this section and the next we will concentrate on understanding the prototypes of those clusters that seem to follow the rule that, the more metal-poor the cluster, the bluer in $B - V$ is the centroid of the horizontal branch.

In Figure 7, *a*, we repeat model tracks for the parameter set already used to infer a spread in stellar mass along the horizontal branch in M3. For better orientation we have added lines of constant stellar radius. The two double lines of "positive" slope roughly define an instability strip within which cluster variables may appear. The blue edge of

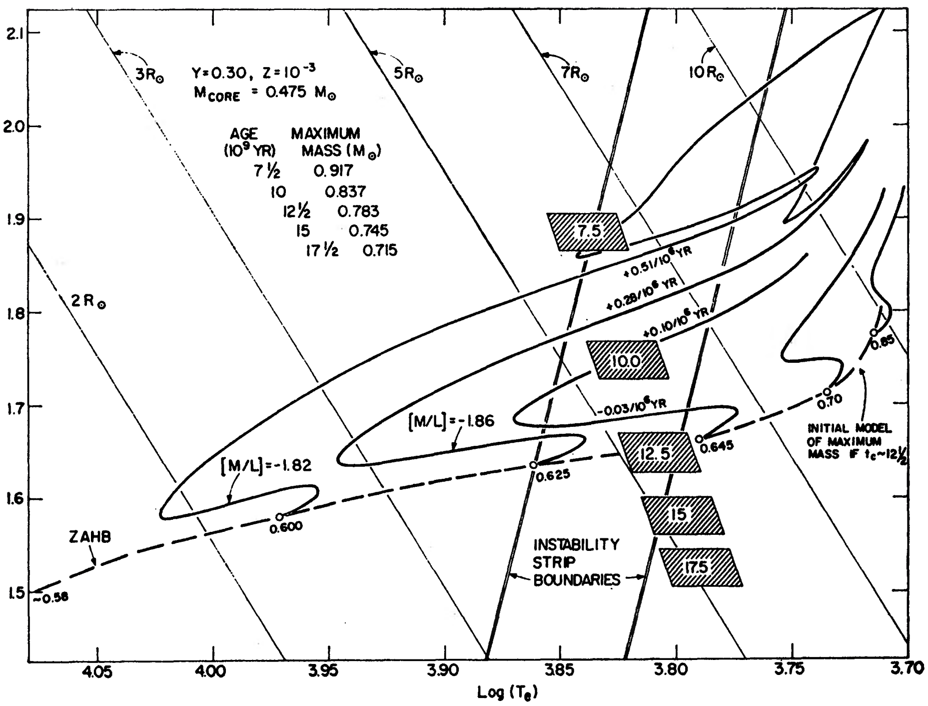

a

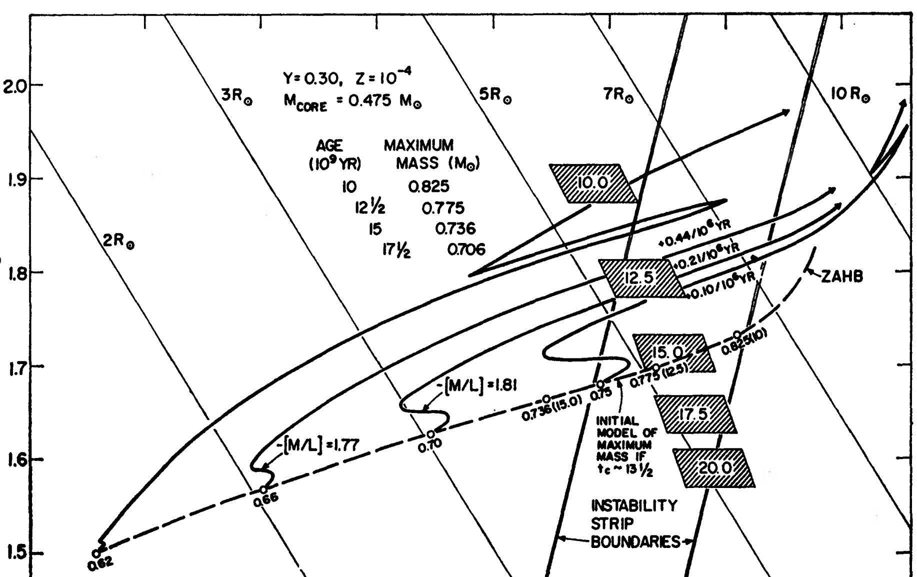

b

FIG. 7.—Additional properties of horizontal-branch models when $Y = 0.3$ and $Z = 10^{-3}$ (Fig. 7, *a*) and $Z = 10^{-4}$ (Fig. 7, *b* and *c*). Lines of constant radius are shown. Double lines mark boundaries of an approximate theoretical instability strip. The center of each shaded square lies exactly 3.4 mag above the theoretical turnoff point along the cluster locus of the indicated age. Slanted table in each figure gives the mass of a model which has just reached the red-giant tip for the first time. The quantity $[M/L] = \log(M/L)$ is indicated at two points in each figure. Beside several tracks evolving to the red through the instability strip are given values of $1.5\, R^{-1}dR/dt$ which describe the models as they reach the center of the strip.

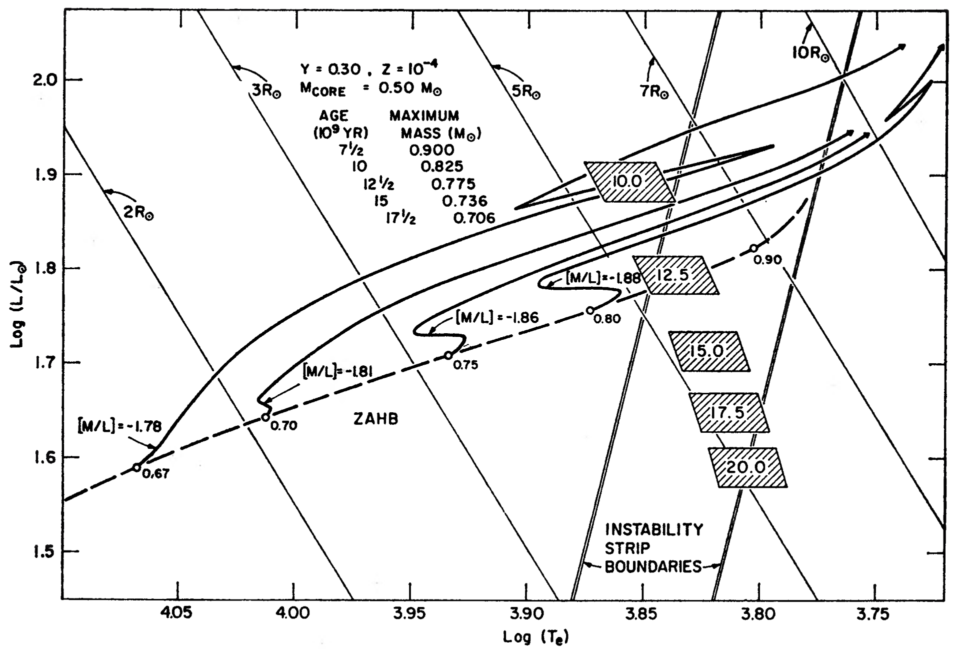

c

FIG. 7.—*Continued*

the strip is taken from Christy's (1966) estimates for $Y = 0.30$ and $M = 0.7\ M_\odot$. The fact that $(\log T_e)_{\rm blue}$ decreases by about 0.01 for every 0.15 $M_\odot$ decrease in stellar mass is of no consequence in the following discussion. The width $\Delta(\log T_e) = 0.06$ of the instability strip is taken from Baker's (1965) estimates.

In the following we shall (*a*) estimate the age of M3 and the maximum possible mass of a horizontal-branch star in M3; (*b*) remark on the wedge shape predicted if a mass dispersion exists; (*c*) compare RR Lyrae luminosities with the observations and with predictions of pulsation theory; and (*d*) suggest additional checks on the adequacy of the theory of stellar interiors.

a) Cluster Age and an Upper Mass Limit

An estimate of the age of M3 and, concomitantly, an estimate of the upper limit on the mass of a horizontal-branch star may be achieved in the following way. In M3, stars at cluster turnoff are dimmer by approximately 3.4 mag than stars of the same color on the horizontal branch. If our theory is correct, we presumably know the absolute luminosity of stars at any point along the horizontal branch and can therefore estimate the luminosity of stars at cluster turnoff. Knowing this latter quantity, we can, on comparison with theoretical time-constant loci, estimate both cluster age and the initial (main sequence) mass $M_{\rm RG}$ of that star which is just reaching the red-giant tip. The estimate is valid only if an average star has lost little mass prior to reaching the turnoff point. If appreciable mass loss occurs near the main sequence, then the age we determine will be an overestimate and we will have underestimated the initial mass $M_{\rm RG}$ (see Clayton 1964). If appreciable mass loss occurs only after the star reaches the giant branch (say, via a steady stellar wind or as a result of shock-induced mass loss accompanying the helium flash), then our estimate of $M_{\rm RG}$ will be approximately correct and will represent the theoretical maximum mass of a horizontal branch star.

In Figure 7, *a*, the center of each box lies directly above the turnoff point of a theoretical time-constant locus of the designated age (see Paper I) by 3.4 mag or by 1.36 in log L. Since the effective temperature of the theoretical turnoff is sensitive to the choice of l/H and since the observational specification of a turnoff point is unavoidably inexact, we have used a box rather than a point. Box width is $\Delta(\log T_e) = 0.03$ and box height is 0.1 mag. The adopted box height underestimates the uncertainty in an observational estimate by a factor of perhaps 2 or 3.

The band defined by joining the blueward-directed portions of individual evolutionary paths gives the region where most horizontal-branch stars should occur. This band lies slightly above the centroid of the box for 12.5×10^9 years. If we have chosen initial core mass and composition properly, we may estimate the age of stars in M3 to be on the order of 11.5×10^9 years.

From the table in Figure 7, *a*, we see that, for this age, $M_{\mathrm{RG}} \sim 0.8\, M_\odot$ is the maximum mass of a horizontal-branch star. Since the track for a model star of any mass greater than about $0.68\, M_\odot$ lies entirely to the red of the adopted instability strip, we may conclude that, unless all stars lose more than about $0.1\, M_\odot$, the region to the red of the RR Lyrae variables should be well populated. This is, of course, the case in M3.

If we were to accept quite literally the mass distribution $\langle N(M)\rangle$ shown in Figure 5, we would conclude that the hydrogen-burning precursor of the average horizontal-branch star (of mass $M \sim 0.64\, M_\odot$) had lost $\sim 0.16\, M_\odot$ during its climb up the giant branch and/or during the helium flash.

It is interesting to compare the conclusions that follow from an admission of a mass spread with those which we would obtain had we adopted the position (Iben and Faulkner 1968) that the horizontal branch must be accounted for by models of a single mass. In the Iben-Faulkner analysis, it is assumed that a single model of the appropriate mass passes directly above cluster turnoff after it has traversed, say, one-quarter of the way along the blueward-directed portion of its path. Inspection of Figure 7, *a*, shows that the appropriate model mass lies somewhere in the neighborhood of $0.65\, M_\odot$. Since the estimate of cluster age is still 11.5×10^9 years (approximately the same RR Lyrae luminosities), we would be forced to conclude that *all* stars lose $\sim(0.80 - 0.65) M_\odot = 0.15\, M_\odot$. We would, of course, be faced with the embarrassment that the track of our single model is distressingly short and incapable of accounting for the observed distribution of stars along the horizontal branch.

From the present vantage point, it is an easy matter to be led by a plausibility argument from the conclusions of the Iben-Faulkner approach to the solution offered in this paper. As long as we are presented with the possibility that at least some stars (those that evolve directly above cluster turnoff) are less massive than their main-sequence precursors, why not accept the possibility that the mass-loss mechanism, whatever it is, is a stochastic process that causes some stars to lose more and some stars to lose less mass regardless of initial mass?

In defense of the Iben-Faulkner approach, we point out that models constructed with earlier approximations to the opacity and earlier estimates of M_C gave track lengths that extended over an interval of roughly 0.2 in log T_e. It did not seem unlikely that better input physics would lead to longer tracks.

b) The Wedge Shape of the Horizontal Branch

It is obvious from Figure 7, *a*, that a distribution of stellar masses along the horizontal branch will produce a "wedge shape" at the blue end in the sense that the luminosity width of the horizontal branch will increase in the direction of increasing $B - V$. Inspection of Figure 1, *c* and *d*, shows that a wedge shape will be produced for any value of (low) Z even if the tracks for the lowest masses evolve only to the red and therefore do not exhibit a blue "hook." If the distribution in mass is relatively continuous, say in the form of a Gaussian about a most probable mass, this wedge will be solid, not "hollow" as it would be if there were no mass spread and if all stars evolved first to the blue and then to the red around a blue hook along the same path in the H-R diagram (Hartwick, Härm, and Schwarzschild 1968). We suspect that the inevitable dispersion that appears in the real world due to differences that lie beyond those permitted by our simplified theory of stellar evolution will always lead to a solid wedge, whether or not a significant mass dispersion exists. Certainly, from the presently available data (e.g., Newell 1970; Newell, Rodgers, and Searle 1969) there is no evidence for a hollow wedge.

c) *RR Lyrae Luminosities*

Our estimate of the luminosity of an RR Lyrae star that lies near the blue edge of the chosen instability strip is somewhat larger than that estimated by Christy (1966) for a variable in M3 that is on the borderline between *c*-type (pulsating in the first harmonic) and *ab*-type (pulsating in the fundamental). Christy finds that the minimum period $P_{\min}$ below which a star cannot pulsate in the fundamental mode seems to be a function of luminosity only. At the critical point (and below) the star can pulsate in the first overtone with a period that is about three-quarters of $P_{\min}$ (or less). Thus, a gap in the distribution of number versus period can lead to an estimate of luminosity at the critical point. Comparing with data for M3, Christy estimates log $(L_{\text{crit}}/L_{\odot}) \sim 1.65$ for such stars. Since our estimate depends strongly on the choice of Z and M_C, and since there are undoubtedly uncertainties in the estimates of pulsation theory as well, we cannot argue that there is a significant discrepancy.

One may also compare the luminosity of an average variable that is suggested by the $Z = 10^{-3}$ models with the average luminosity of field RR Lyrae stars. Pavlovskaya (1953) estimates $\langle M_{\text{pg}} \rangle = 0.5 \pm 0.18$ for 69 RR Lyrae variables; Herk (1965) estimates $\langle M_{\text{pg}} \rangle = 0.87 \pm 0.22$ for 210 variables. If we assume that $\langle M_{\text{bol}} \rangle \sim \langle M_{\text{pg}} \rangle - 0.2$, then Pavlovskaya's average gives $\langle \log L_{\text{RR}} \rangle \sim 1.79 \pm 0.07$ and Herk's average gives $\langle \log L_{\text{RR}} \rangle \sim 1.64 \pm 0.09$. Our estimate of mean L_{RR} for $Z = 10^{-3}$, $\langle \log L_{\text{RR}} \rangle \sim 1.68$, appears to be in agreement, within the uncertainties, with the observational estimates of the luminosity of an average field RR Lyrae star.

d) *Further Checks on the Theory*

Our prediction that blue stars on the horizontal branch in M3 are, on the average, less massive *and* dimmer than red stars on the branch is conceivably susceptible of independent checks. For example, there should be an increase in the mass and luminosity of the *average* RR Lyrae star as one passes from blue to red within the variable instability strip. To first approximation, one might expect that the quantity $Q = P(M/R^3)^{1/2}$ = Period (Mass)$^{1/2}$(Radius)$^{-3/2}$ is the same for all variables pulsating in the same mode. This implies that the potential observable $Q' = P/R^{3/2}$ should be smaller for stars nearer the red edge of the instability strip than for stars nearer the blue edge—as long as attention is confined to one type of variable (just *ab*, for example). Since the width and the position of the appropriate instability strip is not at all well established by the theory, we are justified in making only qualitative estimates. From Figure 7, *a*, we see that model stars in the approximate mass range 0.62–0.67 $M_{\odot}$ spend some time in the chosen instability strip during their blueward motion. There might, therefore, be roughly a 5 percent variation in Q' across the RR Lyrae gap in M3, a variation that might be detected through an analysis of the observational material already available.

Still another check on the prediction of a mass and luminosity dispersion might come from spectroscopic data as interpreted through model atmospheres. In principle one should be able to estimate the *relative* bolometric magnitude of all stars along the horizontal branch and also the ratio M/L for each star. From Figure 7, *a*, and an assumed spread log $T_e \sim 3.76$ to log $T_e \sim 4.15$, we are led to predict a decrease of perhaps 0.5 mag to 0.75 mag in bolometric magnitude and an increase in $\langle [M/L] \rangle$ from ~ -1.9 to -1.7 as one moves from red to blue across the horizontal branch in M3. Here $\langle [M/L] \rangle$ =

$\langle \log (M/L) \rangle$ and the angular brackets denote that an average over the lifetime of a model star has been performed. It is encouraging that the mean value of $[M/L] \sim -1.8 \pm .05$ estimated by Newell (1970) for "cool" horizontal-branch stars in M3 lies within the theoretically estimated spread.

VII. ω CENTAURI, M92, M15, AND LOW-Z MODELS

With the intention of accounting for the characteristics of extremely metal-weak clusters such as ω Cen, M92, and M15, we shall examine the consequences of assuming that models for $Z = 10^{-4}$ and $Y = 0.3$ are appropriate. For illustrative purposes *only*, we assume $M_C = 0.475\ M_\odot$, although, to be consistent with the trend indicated by Eggleton's (1968) work and with our choice of core mass for $Z = 10^{-3}$, we *should* choose $M_C \sim 0.50\ M_\odot$. Model tracks for our illustrative choice of parameters are repeated in Figure 7, *b*. For lack of sufficient theoretical guidance, we choose an instability strip that is identical with the one used to discuss the $Z \simeq 10^{-3}$ case.

The center of each box in Figure 7, *b*, lies 3.4 mag above the turnoff point of a theoretical *t–c* locus of the designated age (for $Y = 0.3$, $Z = 10^{-4}$). This magnitude separation is known to be appropriate for both M92 and M15. Extrapolating from the model tracks in Figure 7, *b*, we conclude that if most stars lying directly above cluster turnoff correspond to models evolving toward the blue, then cluster age is on the order of 14×10^9 years and, from the table in Figure 7, *b*, we find $M_{RG} = 0.75\ M_\odot$. However, stars of this mass do not evolve blueward above the turnoff point.

If, instead, we assume that the stars directly above turnoff are all evolving to the red and that masses of stars that evolve above turnoff are distributed over the range $\sim$0.64–0.75 $M_\odot$, then cluster age (if $M_C = 0.475\ M_\odot$) lies somewhere in the neighborhood of 12.5×10^9 years. But then the maximum theoretical mass of a star on the horizontal branch is in the vicinity of 0.78 $M_\odot$, and such a star evolves on a long time scale directly above turnoff at a luminosity level that would lead to the choice of 14×10^9 years for cluster age.

To resolve the dilemma, we could assume that all stars have lost *at least* 0.03 $M_\odot$. Then all stars of mass $M = M_{RG} - 0.03\ M_\odot$ pass above turnoff only during their luminous redward motion, and the age of 12.5×10^9 years and the theoretical maximum mass $M_{RG} = 0.78\ M_\odot$ are not inconsistent with one another.

For all models of mass less than $\sim$0.75 $M_\odot$, passage through the chosen instability strip is quite rapid relative to the time spent evolving in a region to the blue of the strip. This means that if the distribution in stellar number versus mass is relatively broad and peaks at masses $M \lesssim 0.75\ M_\odot$, most horizontal-branch stars will lie to the blue of the strip with relatively few RR Lyrae stars, and even fewer stars to the red of the strip. This is, of course, actually the case for M92 and ω Cen, and, to a lesser extent, for M15.

Note that the critical point in the Faulkner (1966) sense (the reddest point along the ZAHB) lies far to the red of a second "critical point"—the position on the ZAHB of a model of maximum mass derived by making use of the age implied by the observed luminosity separation between cluster turnoff and horizontal branch. It is clear that all of Faulkner's arguments carry through when one replaces his critical point by this second critical point. In particular, the conclusion that the centroid of the horizontal branch shifts toward the blue with decreasing metallicity (for an appropriate selection of clusters) follows just as in Faulkner's analysis.

In the discussion of M3 we argued that a complete absence of stars in the range $(M_{RG} - 0.1\ M_\odot)$ to M_{RG} would still leave the horizontal branch well populated to the red of the RR Lyrae strip. Such a large minimum mass loss for stars characterized by $Z = 10^{-4}$ would lead to conflict with the distributions along the horizontal branches in M92, ω Cen, and M15. Model stars would all spend most of their lives evolving far to the blue of the RR Lyrae strip. We tentatively suggest that perhaps the degree of mass loss is smaller for stars that are more metal-deficient. This might not be unreasonable if the mass-loss mechanism occurs along the giant branch where, for a given luminosity and mass, metal-deficient stars have a larger surface gravity and smaller convective velocities near the photosphere than do stars that are less metal-deficient. It might also not be unreasonable if shock-induced mass loss occurs during the helium flash and if the violence of the flash increases with increasing metallicity.

A correlation between degree of mass loss (measured by, for example, the difference between M_{RG} and the actual cutoff mass) and metallicity offers a tempting explanation of the "anomalies" presented by M15 and M13 relative to M92, ω Cen, and M3. The latter three clusters follow the rule: the more metal-weak the cluster, the bluer the centroid of the horizontal branch. M15 appears to be roughly as metal-weak as M92 and yet its horizontal branch extends to significantly redder colors; M13 appears to be roughly as moderately metal deficient as M3 and yet the centroid of its horizontal branch lies far to the blue of the centroid of the M3 horizontal branch.

It has been argued that the "classical" order represented by M92, ω Cen, and M3 is related to the fact that a "critical point" along a theoretical horizontal branch (Faulkner 1966; this paper) moves to the blue as Z is decreased. Observational exceptions to the classical order obviously point to an additional parameter or parameters not taken into account in the two definitions of a critical point thus far offered. Could an additional parameter be the degree of mass loss?

Let us define a third critical point as that location on the ZAHB of a model having the mass of an average horizontal-branch star. All other things being equal, the greater the degree of mass loss assumed, the farther to the blue will this third critical point lie. For a given degree of mass loss, the third critical point will, of course, move to the red as Z is increased. Thus, if we assume that the degree of mass loss increases with Z, the position of the third critical point will be determined by two competing effects that work in opposite directions.

A satisfactory ordering of the known facts results if we assume that the mass-loss effect loses out at "low" Z but wins at "high" Z, thus leading to the possibility that two different values of Z can be associated with third critical points that have the same color coordinate. Adopting this solution, we would predict that, when written in the order M15, M92, ω Cen, M3, M13, the average horizontal-branch star in each successive cluster is more metal-rich and has suffered more mass loss than the average horizontal-branch star in the previous one.

Checks on the prediction of a spread in mass and luminosity along the horizontal branch in low-Z clusters can be devised as before. If the situation is as depicted in Figure 7, *b*, so that most RR Lyrae stars of long period are evolving to the red, then there will be little or no correlation between the mass and color of variable stars of type *ab*. Since the dispersion in luminosity of stars passing to the right through the strip is so small, one would also not expect a very strong correlation between the magnitude and mass of type *ab* variable stars. There should, however, be a pronounced dispersion in mass. Since the speed of passage through the strip is greater for stars of lower mass, one might predict a preponderance of higher masses.

A slight increase in Z or a shift of the instability strip toward the blue can alter the situation in such a way that the RR Lyrae phase usually coincides with the dominant blueward phase of evolution. A study of mass dispersion in the RR Lyrae region of M92, ω Cen, and M15 could conceivably distinguish which of the two descriptions best represents them.

The values of $\langle [M/L] \rangle$ for model tracks in Figure 7, *b*, range from about -1.85 near the blue edge of the instability strip to -1.69 near $\log T_e \sim 4.1$, while stellar mass varies from about $0.75\ M_\odot$ to about $0.61\ M_\odot$. The values of the mass-to-light ratio near the blue end are about a factor of 2 larger than those estimated by Newell, Rodgers, and Searle

(1969) for the bluest stars in ω Cen. We remark that these authors find a spread in $[M/L]$ that extends from -2.27 to -1.59 and estimate a spread in individual masses between 0.28 and 1.12 $M_{\odot}$. We would find it hard to account theoretically for the horizontal branch with such a large spread in masses and suggest that most of the derived spread is a measure of the uncertainty in the analysis. Our results are then not in conflict with the observations on ω Cen.

Comparison should also be made with Newell's (1970) analysis which gives $\langle[M/L]\rangle = -1.81 \pm 0.26$ and $\langle[M/L]\rangle = -2.08 \pm 0.14$ for "hot blue horizontal branch" stars in M15 and in M92, respectively. For "cool blue horizontal branch" stars in M15 and M92, Newell gives $\langle[M/L]\rangle = -1.78 \pm 0.10$ and $\langle[M/L]\rangle = 1.90 \pm 0.07$, respectively. One might infer that the "observed" variation in M/L with color is just the opposite to that predicted by the theory. However, as Newell cautions, since the analysis is different in the "hot" and "cool" cases, the "hot" and "cool" results cannot be directly intercompared. The best we can conclude is that our theoretical estimates of M/L are not inconsistent with Newell's estimates.

Slightly smaller theoretical values of $\langle[M/L]\rangle$ and smaller cluster ages result if instead of $M_C = 0.475\ M_{\odot}$ we choose $M_C = 0.50\ M_{\odot}$, as suggested by Eggleton's (1968) results when $\epsilon_{\nu\nu} \neq 0$. In Figure 7, *c*, we give the appropriate ZAHB and sketch estimates of the appropriate tracks. Now, cluster age is estimated at 11×10^9 years, and $\langle[M/L]\rangle$ varies between -1.87 and -1.76 over the range $\log T_e \sim 3.85$ to $\log T_e \sim 4.10$.

In closing, we compare luminosity near the blue edge of the instability strip with that derived by Christy (1966) for M15 and ω Cen. Christy estimates $\log (L/L_{\odot}) \sim 1.66$ for the bluest *ab* type RR Lyrae stars in both clusters. Our estimate from Figure 7, *b*, is $\log (L/L_{\odot}) \sim 1.70$, whereas from Figure 7, *c*, it is $\log (L/L_{\odot}) \sim 1.77$, the latter being our favored choice. Again, as in the case of M3, our estimate is higher than Christy's. Note, however, that our estimates vary with the degree of metallicity in the same way that Christy's do: the higher the value of Z, the lower the luminosity of RR Lyrae variables at the blue edge of the instability strip. The fact that the same trend follows from a comparison between the observations and pulsation theory as well as from a self-consistent theory of stellar evolution permits one to hope that the slight disparity in quantitative predictions will be reduced once all uncertainties in both pulsation theory and evolutionary theory have been properly assessed.

VIII. COMMENTS ON PERIOD CHANGES OF RR LYRAE VARIABLES

Secular variations in the period of a cluster variable are to be expected as a result of evolutionary changes in mean stellar radius. A theoretical estimate of the rate at which period might be expected to change is easily achieved. In first approximation, period, mass, and radius are related by $P \propto M^{-1/2}R^{3/2}$ so that, for fixed stellar mass, $P^{-1}dP/dt \simeq \frac{3}{2}R^{-1}dR/dt$. In Figure 8 (see also Fig. 3, *a*) we plot this latter quantity versus time for a selection of horizontal-branch models characterized by the parameter set $Z = 10^{-3}$, $Y = 0.3$, $M_C = 0.475\ M_{\odot}$, which we have assumed to be appropriate for understanding the cluster M3.

We see that, for those models ($M/M_{\odot} \sim 0.64$–0.67) that spend a large fraction of their core-helium-burning lifetime evolving toward the blue through the instability strip, the instantaneous value of $-P^{-1}dP/dt$ never exceeds $0.05/10^6$ years. For these stars, the time average of $-P^{-1}dP/dt$ during blueward motion within the strip is less than $0.02/10^6$ years. Since RR Lyrae periods are typically in the range (0.5–1) day, these limits are true also of dP/dt in units of days per million years. For those model stars ($M/M_{\odot} < 0.66$) that spend a large fraction of their lives evolving to the red through the instability strip during core helium burning, $P^{-1}dP/dt$ remains below $0.05/10^6$ years during redward evolution and the time average is even less than this. Only for those models ($M/M_{\odot} < 0.63$) that reach the strip for the first time after evolving first to the blue does $P^{-1}dP/dt$ exceed $0.2/10^6$ years, but the time spent in the strip during core helium burning is quite short compared with the total horizontal-branch lifetime.

The high abundance of RR Lyrae stars in M3 relative to redder and bluer horizontal-branch stars suggests that most variables in M3 are evolving within the instability strip on a long time scale. This permits us to make another estimate of the upper limit on average $P^{-1}dP/dt$ that does not depend sensitively on model details. At a mean luminosity level of $\langle \log L_{RR} \rangle \sim 1.67$, stellar radius differs by $\Delta(\ln R) \sim 0.28$ from one edge to the other of the instability strip shown in Figure 7, *a*. The average core-helium-burning lifetime of a model with $M_C = 0.475\, M_\odot$ is $t_{HB} \sim 6.3 \times 10^7$ years. If we assume that the average track length during blueward evolution is similar to that of the 0.625

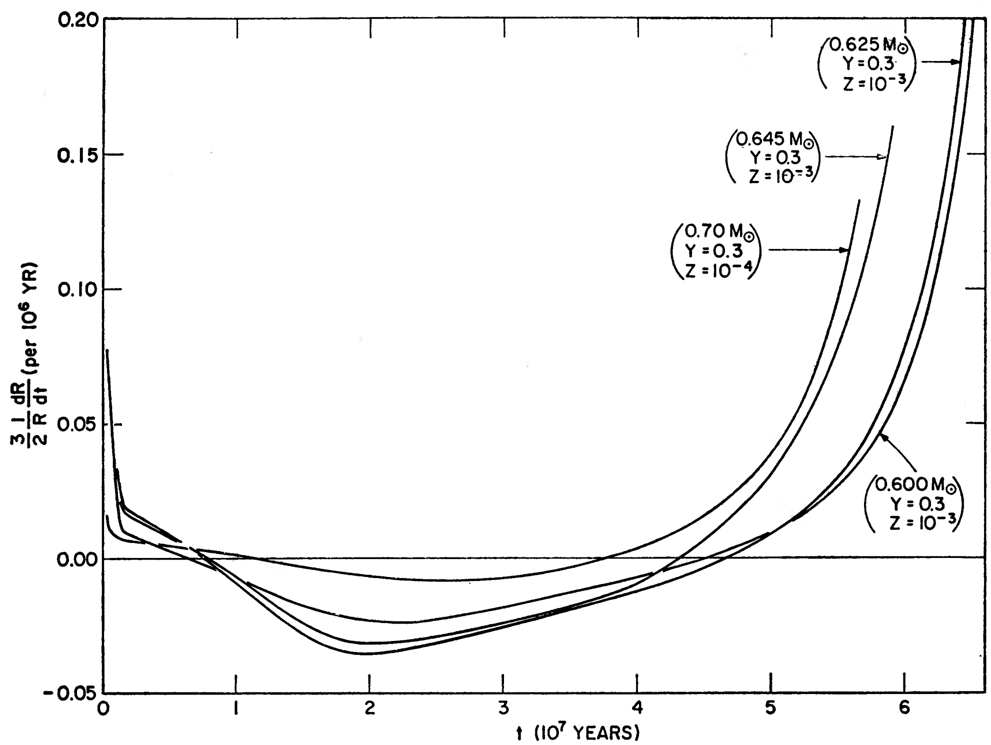

FIG. 8.—Logarithmic rate of change of stellar radius during core helium burning for several models with $M_C = 0.475\, M_\odot$ and $Y = 0.3$. Stellar mass in units of the solar mass and the parameter Z are designated.

$M_\odot$ star in Figure 7, *a* (i.e., roughly one-quarter of the width of the horizontal branch in M3), then $\langle P^{-1}dP/dt \rangle \sim -(\frac{3}{2} \times 0.28)/(6.3 \times 10^7 \text{ years}) \sim -0.007/10^6$ years is a measure of an average negative rate of period change. If we assume instead that the average blueward track length is comparable to the width of the M3 horizontal branch, then we obtain $\langle P^{-1}dP/dt \rangle \sim -0.03/10^6$ years as an upper limit.

Another quantity that can be compared with the observations on rates of change of period is the probability that the radius of a star within the instability strip is either increasing or decreasing. For those models ($Y = 0.3, Z = 10^{-3}$) that spend the greatest fraction of their core-helium-burning lives in the instability strip, the time spent evolving to the red is roughly one-third the time spent evolving to the blue. Consequently, for almost any distribution in stellar number versus stellar mass, the quantity $N_+/N_- =$ (number with increasing period)/(number with decreasing period) would be $\sim\frac{1}{3}$. Comparing the tracks and evolutionary rates in Figure 1, *a*, with those in Figure 1, *b*, shows that a decrease in Z below 10^{-3} would cause N_+/N_- to increase. This is obvious also from the fact that, when current estimates of M_C are adopted, all models for $Y < Y_I \sim 0.25$ (when $Z = 10^{-3}$) or 0.28 (when $Z = 10^{-4}$) evolve only to the red during core helium burning.

We are now in a position to compare with the observations. An estimate of the rate at which periods change for stars in the cluster M3 was first made by Martin (1942) and by Hett (1942) and later by Belserene (1952) and by Roberts and Sandage (1955). In Figure 9 we display the distribution in number versus dP/dt found by Martin for a selection of *ab* variables.

The high frequency of decreasing periods (in fact, $N_+ \sim N_-$) might be taken as corroboration of the high-helium hypothesis since only those stars with $Y > Y_I \sim 0.25$ evolve toward the blue during core helium burning. However, if one averages over the negative dP/dt portion of the distribution, one obtains $\langle -(dP/dt)\rangle$ blue $\sim$0.2 day/10^6

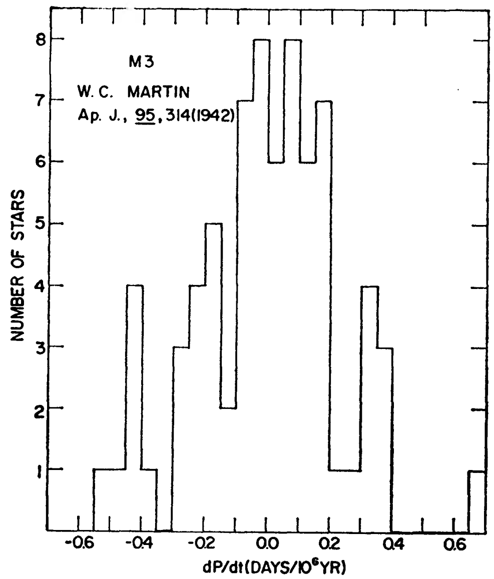

FIG. 9.—Distribution in number versus rate of period change for variables in M3

years, a value that is an order of magnitude larger than that just estimated theoretically for $Y = 0.3$, $Z = 10^{-3}$.

We tentatively conclude that rates of change of period estimated in the manner of Martin and others are not a measure of the rates at which stars evolve (as a consequence of nuclear burning in their interiors) through the instability strip. However, if we are unable to provide an alternative theoretical explanation for the derived changes in period, we cannot rule out the possibility that our models are grossly in error.

In Figure 10 we show the location in the color-magnitude diagram of those stars in M3 for which both period-change estimates and photometry are available. With the exception of the luminous stars near the red edge of this sample, there seems to be no clear-cut correlation between position in the color-magnitude diagram and the sign of a period-change rate. In contrast, all of the luminous, red stars that form the upper right-hand portion of the distribution in Figure 10 are increasing in period. We have seen that, during the major part of their core-helium-burning lives, $[\langle dP/dt\rangle]_{\text{evolution}} \ll [\langle dP/dt\rangle]_{\text{observed}}$. However, after rounding the blue-hook portion of the evolutionary path, $R^{-1}dR/dt$ becomes increasingly more positive, reaching values that are comparable to observed mean changes. We could achieve consistency with the observation if some cause other than evolutionary changes in radius led to apparently random changes in period that mask any evolution-related changes occurring during most of a star's life on the horizontal branch but become comparable to evolution-related changes during phases of more rapid change near the end of core helium burning.

Without pretending to understand its origin, let us call the major contribution to a typical observed dP/dt "noise." The near equality of N_+ and N_- and the rough symmetry of the observed distribution about the origin in Figure 9 is explained by assuming that the noise is random and that the average contribution of evolutionary changes to the distribution is small compared with the noise. A slight bias toward positive values of dP/dt ($\langle dP/dt \rangle \sim +0.03$ days/10^6 years for the distribution in Fig. 9) is attributable

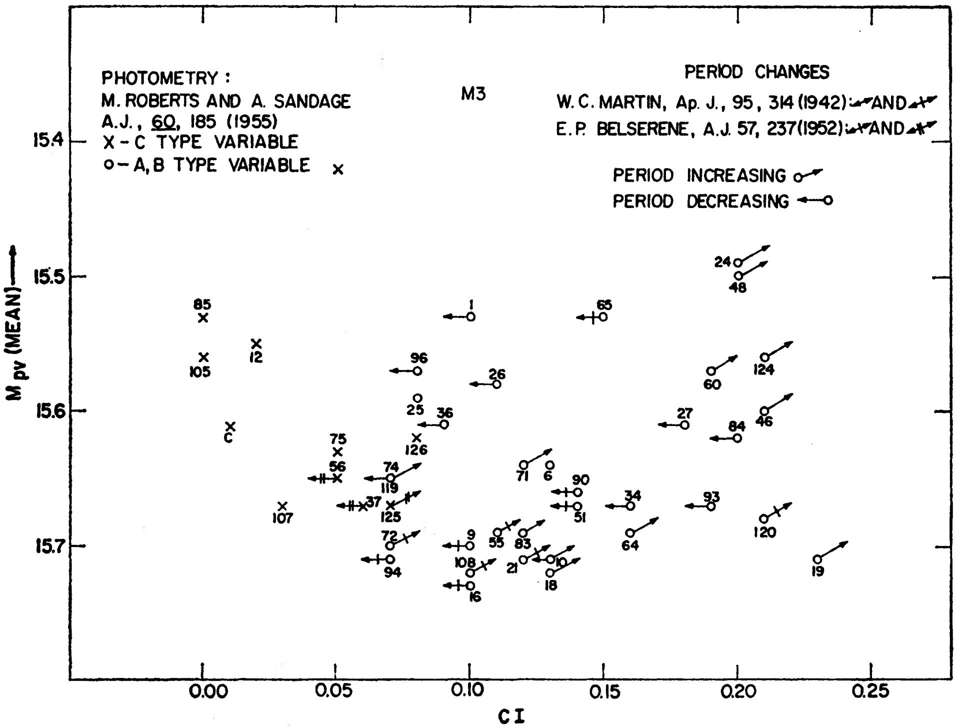

FIG. 10.—Distribution of rates of period change in the C-M diagram. Arrows pointing upward and to the right mean $dP/dt > 0$. Arrows pointing to the left mean $dP/dt < 0$.

to the fact that negative contributions to dP/dt due to evolutionary changes in radius are always small in absolute value compared with the observed rates whereas positive values of dP/dt due to evolutionary changes can become comparable to observed rates.

Rates of period change estimated from calculations with $Z = 10^{-4}$ can also be compared with the observations. We have argued that, if models characterized by the parameter set $Y = 0.3$, $Z = 10^{-4}$, $M_C > 0.475\ M_\odot$ describe stars in clusters such as M92 and ω Cen, then most of the RR Lyrae stars in these clusters are evolving to the red after having completed a major portion of their core-helium-burning lives. Adopting the same instability strip as that in Figure 7, we have calculated, as a function of stellar mass, time-average values of $P^{-1}dP/dt$ for those portions of a star's track that pass redward through the instability strip during core helium burning. The results for three masses are shown next to the appropriate paths in Figure 7, *b*.

For comparison we show in Figure 11 the distribution in number versus rate of period change derived by Belserene (1964) for several *ab*-type stars in ω Cen. This distribution, as well as that derived by Wright (1940), confirms the findings of Martin (1938). We note at once the rough symmetry of the distribution about a positive value of $dP/dt \sim 0.1$. The symmetry would be expected if the positive and negative "noise" contributions were equally frequent and random. We infer from the magnitude of the bias toward positive values of dP/dt that most of the RR Lyrae stars are evolving from blue to red through the instability strip, just as we have anticipated with the help of the $Z = 10^{-4}$ models. The mean value of $\sim +0.1$ day/10^6 years in the observed distribution is consistent with the values we have estimated from the theory.

We are very grateful to Cecelia Payne-Gaposchkin for introducing us to the literature on changes in RR Lyrae periods.

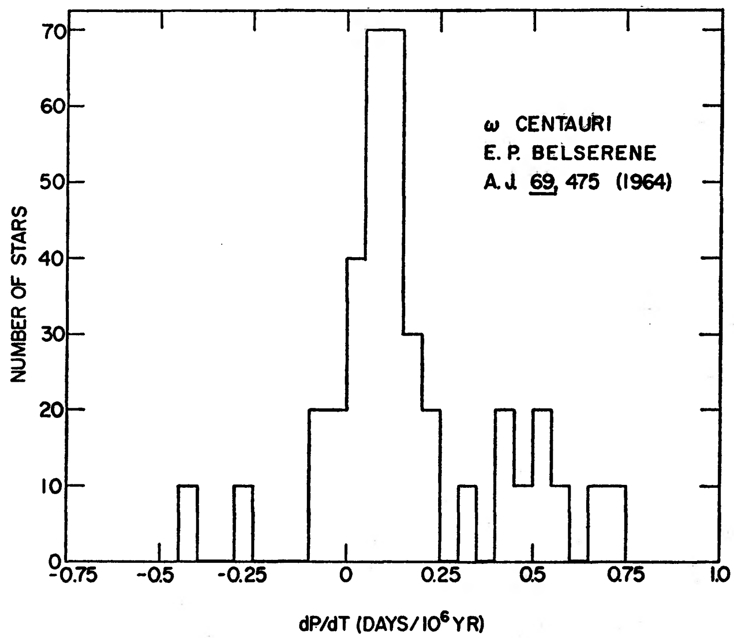

FIG. 11.—Distribution in number versus rate of period change for variables in ω Cen

REFERENCES

Baker, N. H. 1965, *Bamberger Veroff.*, **4**, 122.
Belserene, E. P. 1952, *A.J.*, **57**, 237.
———. 1964, *ibid.*, **69**, 475.
Christy, R. F. 1966, *Ap. J.*, **144**, 108.
Clayton, D. D. 1964, *Ap. J.*, **140**, 1604.
Cox, A., and Stewart, J. 1970, *Ap. J. Suppl.*, No. 174, **19**, 261.
Edwards, A. C. 1970, *M.N.R.A.S.*, **146**, 445.
Eggen, O. J., Lynden-Bell, D., and Sandage, A. R. 1962, *Ap. J.*, **136**, 748.
Eggleton, P. P. 1968, *M.N.R.A.S.*, **140**, 387.
Faulkner, J. 1966, *Ap. J.*, **144**, 978.
Faulkner, J., and Iben, I., Jr. 1966, *Ap. J.*, **144**, 995.
Hartwick, F. D. A., Härm, R., and Schwarzschild, M. 1968, *Ap. J.*, **151**, 389.
Herk, G. van. 1965, *B.A.N.*, **18**, 71.
Hett, J. H. 1942, *A.J.*, **50**, 77.
Iben, I., Jr. 1968, *Ap. J.*, **154**, 581.
———. 1968, *Nature*, **220**, 143.
Iben, I., Jr., and Faulkner, J. 1968, *Ap. J.*, **153**, 101.
Iben, I., Jr., and Rood, R. T. 1969, *Nature*, **223**, 933.
———. 1970, *Ap. J.*, **159**, 605 (Paper I).

Iben, I., Jr., Rood, R. T., Strom, K. M., and Strom, S. E. 1969, *Nature*, **224**, 1008.
Martin, W. Chr. 1938, *Leiden Ann.*, Vol. **17**, Part II.
———. 1942, *Ap. J.*, **95**, 314.
Newell, E. B. 1970, *Ap. J.*, **159**, 443.
Newell, E. B., Rodgers, A. W., and Searle, L. 1969, *Ap. J.*, **158**, 699.
Ohyama, N. 1963, *Progr. Theoret. Phys.*, **30**, 170.
Ono, Y., and Sakashita, S. 1961, *Pub. Astr. Soc. Japan*, **13**, 146.
Pavlovskaya, E. D. 1953, *Peremenniye Zvezdy*, **9**, 349.
Peebles, P. J. E., and Dicke, R. H. 1968, *Ap. J.*, **154**, 891.
Roberts, M., and Sandage, A. R. 1955, *A.J.*, **60**, 185.
Rood, R. T. 1970, *Ap. J.*, **161**, 145 (Paper II).
Rood, R. T., and Iben, I., Jr. 1968, *Ap. J.*, **154**, 215.
Sakashita, S., and Tanaka, Y. 1962, *Progr. Theoret. Phys.*, **27**, 127.
Sandage, A. R. 1969, *Ap. J.*, **157**, 515.
Schwarzschild, M., and Härm, R. 1962, *Ap. J.*, **136**, 158.
———. 1964, *ibid.*, **139**, 594.
———. 1966, *ibid.*, **145**, 496.
Searle, L., and Rodgers, A. W. 1966, *Ap. J.*, **143**, 809.
Stephensen, G. J., Jr. 1966, *Ap. J.*, **146**, 950.
Sugimoto, D. 1964, *Progr. Theoret. Phys.*, **32**, 703.
Thomas, H-C. 1967, *Zs. f. Ap.*, **67**, 420.
Wagoner, R. V., Fowler, W. A., and Hoyle, F. 1967, *Ap. J.*, **148**, 3.
Watson, W. D. 1969*a*, *Ap. J.*, **157**, 375.
———. 1969*b*, *ibid.*, **158**, 303.
Woolf, N. J. 1964, *Ap. J.*, **139**, 1081.
Wright, F. W. 1940, *Harvard Bull.*, No. 912, p. 8.